Arbeitsbericht NAB 22-07

HotBENT Project – Bentonite Materials Requirements and Production

December 2022

R. Schneeberger, F. Kober,
S. Kaufhold & R. Dohrmann

National Cooperative for the Disposal of Radioactive Waste

Hardstrasse 73
P.O. Box
5430 Wettingen
Switzerland
Tel. +41 56 437 11 11

nagra.ch

nagra.

Arbeitsbericht NAB 22-07

HotBENT Project – Bentonite Materials Requirements and Production

December 2022

R. Schneeberger[1], F. Kober[1],
S. Kaufhold[2] & R. Dohrmann[2]

[1] Nagra
[2] Bundesanstalt für Geowissenschaften und Rohstoffe - BGR

KEYWORDS
GTS Phase VI, HotBENT, Bentonite, Emplacement, Engineered Barrier System

National Cooperative for the Disposal of Radioactive Waste

Hardstrasse 73
P.O. Box
5430 Wettingen
Switzerland
Tel. +41 56 437 11 11

nagra.ch

Nagra Arbeitsberichte ("Working Reports") present the results of work in progress that have not necessarily been subject to a comprehensive review. They are intended to provide rapid dissemination of current information.

Table of Contents

Table of Contents I

List of Tables III

List of Figures IV

List of Acronyms VI

1 Introduction 1
1.1 HotBENT in brief 1
1.2 Timeline of on-site activities and scope of the report 3
1.3 History of the HotBENT experiment and scope of this report 4

2 Raw bentonite materials 5
2.1 Introduction 5
2.2 Requirements 5
2.3 Bentonite materials used for HotBENT 5
2.3.1 Na-dominated Wyoming-type bentonite (National® WP1000) 5
2.3.2 Bentonite Černý Vrch (BCV) 7

3 Bentonite blocks 9
3.1 Introduction 9
3.2 Design requirements 9
3.3 Pre-production test for BCV ordinary blocks 10
3.3.1 Manufacturing 10
3.3.2 Quality control 10
3.4 Block production for HotBENT 13
3.4.1 Water content adjustments 13
3.4.2 Manufacturing 14
3.4.3 Quality control and characterisation of the blocks 14
3.4.3.1 At the factory 14
3.4.3.2 At GTS 17

4 Granular bentonite material (GBM) 21
4.1 Manufacturing and quality control 21
4.2 Pelletisation 22
4.3 Mixing and rounding 25
4.4 Packaging and transport 27
4.5 Quality control at GTS 28

5 Emplacement in HotBENT 29
5.1 Emplacement of the bentonite blocks in HotBENT 29
5.2 Emplacement of GBM in HotBENT 31
5.2.1 Backfilling unit and procedure 31
5.2.2 Emplacement slopes (ES) 33
5.2.3 Backfilled volumes 33

5.2.4 Backfilled mass of GBM 34
5.2.5 Backfilled GBM density 34
5.2.6 Water content of emplaced GBM 35
5.2.7 Backfilled dry density of the GBM 36
5.2.7.1 Backfilling procedure of GBM behind retaining wall 38
5.2.8 General observations during backfilling 40

6 Baseline characterisation 41
6.1 Sample preparation 41
6.1.1 GBM samples 41
6.1.2 Block samples 41
6.2 Chemical analyses (XRF + LECO) of GBM samples 42
6.3 Block samples 51

7 Lessons learned and conclusions 53
7.1 Blocks 53
7.2 GBM 53
7.3 Summary of baseline characterisation 53
7.4 Conclusions 54

8 References 57

List of Tables

Tab. 2-1: Raw material requirements for the Wyoming-type bentonite (Garitte et al. 2015) 5
Tab. 2-2: Characteristics of National® 1802 as indicated by the supplier 6
Tab. 2-3: Characteristics of BCV as indicated by SURAO (Hausmannová et al 2018) 7
Tab. 3-1: Geometric quality control on the pre-production blocks at the factory 11
Tab. 3-2: Water content measurements on pre-production BCV ordinary blocks at GTS 13
Tab. 3-3: Quality control on National® 1802 ordinary blocks at the factory 15
Tab. 3-4: Quality control on National® 1802 top blocks at the factory 16
Tab. 3-5: Uniaxial compressive strength measured on the produced blocks at the factory 16
Tab. 3-6: Water content measurements on the bentonite blocks after delivery to the GTS 17
Tab. 3-7: Dry density values for bentonite blocks 19
Tab. 5-1: Weight of each heater bentonite block pedestal 30
Tab. 5-2: Backfilling steps with emplaced mass of GBM and backfilled volume 35
Tab. 5-3: Water content values for emplaced GBM 36
Tab. 5-4: Emplacement dry density values for GBM per emplacement step and at selected intervals 37
Tab. 6-1: Average compositions of GBM samples based on XRF and LECO data 50
Tab. 6-2: Comparison of the average values of chemical analyses of the National® GBM samples (upper row) with the average values of the National® block samples 52
Tab. 6-3: Comparison of the chemical composition of all (n=23) BCV GBM samples (BCV, upper row) with top and ordinary blocks 52
Tab. 7-1: Summary of bentonite components in HotBENT 55

List of Figures

Fig. 1-1: Layout of HotBENT test (current design): A) vertical section, B) plan view showing HotBENT cavern ... 2

Fig. 1-2: Overall timeline for the on-site implementation of HotBENT ... 3

Fig. 2-1: Grain-size distribution of the raw material National® WP1000 ... 6

Fig. 3-1: Shapes of bentonite block required for the bentonite block pedestals ... 9

Fig. 3-2: Relative humidity evolution in the VE cavern and the BK cavern over 1 month ... 12

Fig. 3-3: Equilibrium relative humidity of the BCV blocks ... 12

Fig. 3-4: Impressions from the bentonite block manufacturing ... 14

Fig. 3-5: Allowed maximum damages in the blocks after production ... 15

Fig. 3-6: Water content measurements in the bentonite blocks after delivery to the GTS ... 18

Fig. 4-1: Dry density of a pellet mixture as function of the pellet dry density and the inter-pellet porosity ... 21

Fig. 4-2: Water content of National® WP1000 raw material used for GBM manufacturing ... 22

Fig. 4-3: Process of pelletisation (modified after Hofmann et al. 2007) ... 23

Fig. 4-4: Quality control after pelletisation ... 24

Fig. 4-5: Pictures of the different bentonite products during GBM manufacturing ... 25

Fig. 4-6: Histogram showing loose density (dry and wet) for the National® WP1000 and BCV GBM ... 26

Fig. 4-7: Sieve curve analysis of GBM after production ... 26

Fig. 4-8: Impressions from the packaging of the GBM ... 27

Fig. 4-9: Transport of the GBM big bags to the Grimsel Test Site ... 27

Fig. 4-10: Evolution of relative humidity and temperature in the vicinity of GBM big bag number 1 of National® WP1000 ... 28

Fig. 4-11: Equilibrium relative humidity for the National® 1802 and BCV ordinary and top blocks and the GBM ... 28

Fig. 5-1: Bentonite block arrangement in the heater pedestals ... 29

Fig. 5-2: Impressions from the construction of the bentonite block pedestal ... 30

Fig. 5-3: Graphical visualisation of the backfilling unit with the five-auger machine in front and the feeder wagon with four bentonite big bags behind ... 31

Fig. 5-4: Impressions from backfilling ... 32

Fig. 5-5: Typically backfilled slopes around the heater (left) and without the heater (right) ... 32

Fig. 5-6: Examples of emplacement slope surveying ... 33

Fig. 5-7: GBM emplacement slopes along an axis-parallel cross-section ... 33

Fig. 5-8: Water content of emplaced GBM ... 36
Fig. 5-9: Impressions from the backfilling procedure behind the retaining wall ... 39
Fig. 5-10: Air escape during backfilling... 40
Fig. 6-1: Photographs of all blocks sent to BGR (left) as well as sampling of each block (right) ... 42
Fig. 6-2: LOI values of all GBM samples ... 43
Fig. 6-3: TiO_2 contents of all GBM samples ... 44
Fig. 6-4: Fe_2O_3 contents of all GBM samples ... 45
Fig. 6-5: S contents of all GBM samples ... 46
Fig. 6-6: Organic C contents of all GBM samples ... 47
Fig. 6-7: Inorganic C contents of all GBM samples... 48
Fig. 6-8: CaO contents of all GBM samples ... 49
Fig. 6-9: Comparison of the chemical composition of the 12 block samples... 51
Fig. 6-10: Differences between BCV top and ordinary blocks ... 52

List of Acronyms

Example:

BCV	Bentonite Černý Vrch
BK	Bohrkranz cavern at GTS
EGPB	Enhanced geosphere pressurisation boreholes
ERT	Electrical resistivity tomography
ES	Emplacement slope
FE	Full-scale Emplacement experiment at Mont Terri
FEBEX	Full-scale Engineered Barrier System Experiment
GBM	Granular bentonite material
GTS	Grimsel Test Site
H	Heater
KAN	National® standard samples shipped to Canada
LOI	Loss on ignition
NAS	National® standard
NWMO	Nuclear Waste Management Organisation in Canada
OB	Ordinary block
Org	Organic
Ref	Reference
RH	Relative humidity
RW	Retaining wall
St. Dev.	Standard deviation
TB	Top block
THM	Thermo-hydro-mechanical
TM	Tunnel metre
VE	Ventilation cavern at GTS
WP	Work package
XRD	X-Ray diffraction
XRF	X-Ray fluorescence

1 Introduction

This report is part of a series of reports documenting the implementation of the HotBENT project (Schneeberger et al. 2021, Schneeberger and Kober 2022 and Kober et al. in prep). The design and background information of the HotBENT project are described in more detail in Kober et al. (2018) and Nagra (2020).

1.1 HotBENT in brief

Enlarging the understanding and databases on the behaviour of clay-based engineered barrier systems (EBS) under high temperatures (i.e., beyond 150 °C at the heater surface) has been motivated by the required information for repository optimisation with respect to design, space and costs (e.g. footprint, layout), as well as increasing the options regarding the required interim storage time or waste packaging.

The performance of bentonite barriers in the ~100 °C temperature range is underpinned by a broad knowledge base built on modelling, laboratory and large-scale in-situ experiments (see summary Kober et al. 2018). The HotBENT experiment follows along the lines of previously completed heater experiments by various waste management organisations in several underground research facilities (with different types of host rock) for characterising the THM-C behaviour (thermo-hydro-mechanical-chemical) of clay buffers and demonstrating the feasibility of constructing reference repositories, such as FEBEX (ENRESA 2000, Kober et al. 2021), HE-E (Gaus et al. 2014), TBT (Åkesson 2012), Prototype Repository (Svemar et al. 2016) or FE (Müller et al. 2017, Nagra 2019).

Characterisation of bentonite parameters above 100 °C is sparse (especially for pelletised materials), although no significant changes in safety-relevant properties are indicated up to about 150 °C (Leupin et al. 2014). HotBENT will contribute to closing this knowledge gap by

- studying the effects of high temperatures (high thermal loading) (> 150 ºC) at and in the vicinity of the heater surface on the performance of bentonite and/or bentonite mixtures as buffer materials considering repository-relevant scales and under in-situ conditions
- enhancing the existing databases and the understanding of buffer performance under such high temperatures, in particular in terms of robustness with respect to assessing the effect on the generally agreed safety functions
- investigating the chemical behaviour that can be described with the models and data from existing, albeit limited and in part ambiguous, laboratory-scale investigations at higher temperatures
- scrutinising whether current conceptual and numerical models have sufficient predictive power (i.e. including uncertainty range) to understand the experiment and describe the prevailing processes
- evaluating whether buffer alteration does occur, and if so, to what extent it (significantly) affects accepted safety functions and requirements

Additional aims to maximise added value from the project are:

- evaluating corrosion of potential canister materials (by means of corrosion coupons)
- evaluating microbial activity (and its effects on e.g. the buffer/canister)
- considering the interaction of bentonite buffer with cement-based liners and/or plugs

The constructed HotBENT experiment consists of four heaters in two sectors with an intermediate and a terminal plug as is shown in Fig. 1-1.

- Test Sector 2: Tunnel metres I 37.7-54.25 with BCV and Wyoming-type bentonite modules
- Test Sector 1: TM 57.75-70 with two Wyoming-type modules (one with four metres of liner at the back end, TM–66 - 70)

The construction of two sectors will allow the partial dismantling of Sector 2 (planned after 5 years of heating) without perturbation of the ongoing further evolution (hydration/saturation) in Sector 1, which is due for dismantling after a heating and hydration phase of about 20 years, as modelling indicated that these timescales are needed for the ambient conditions at the Grimsel Test Site (GTS). Two different bentonites were used: widely studied Wyoming type bentonite (National® Standard) and the Czech bentonite BCV (Bentonite Černý Vrch). Both were emplaced in the form of compacted bentonite blocks for heater pedestals and as granular bentonite material (GBM) to fill the void between the heaters and the gallery walls.

In addition to the heater modules and the backfill inside the former FEBEX gallery (Enresa 2000, Kober et al. 2021, Fig. 1-2), the experimental concept includes four water-filled, enhanced geosphere pressurisation boreholes running sub-parallel to the gallery (Lanyon et al. 2019, Schneeberger and Rouspoulou 2021). The boreholes are dedicated to increasing the hydraulic pressure in the geosphere and thus the hydraulic gradient towards the experiment (Lanyon et al. 2019, Schneeberger et al. 2021).

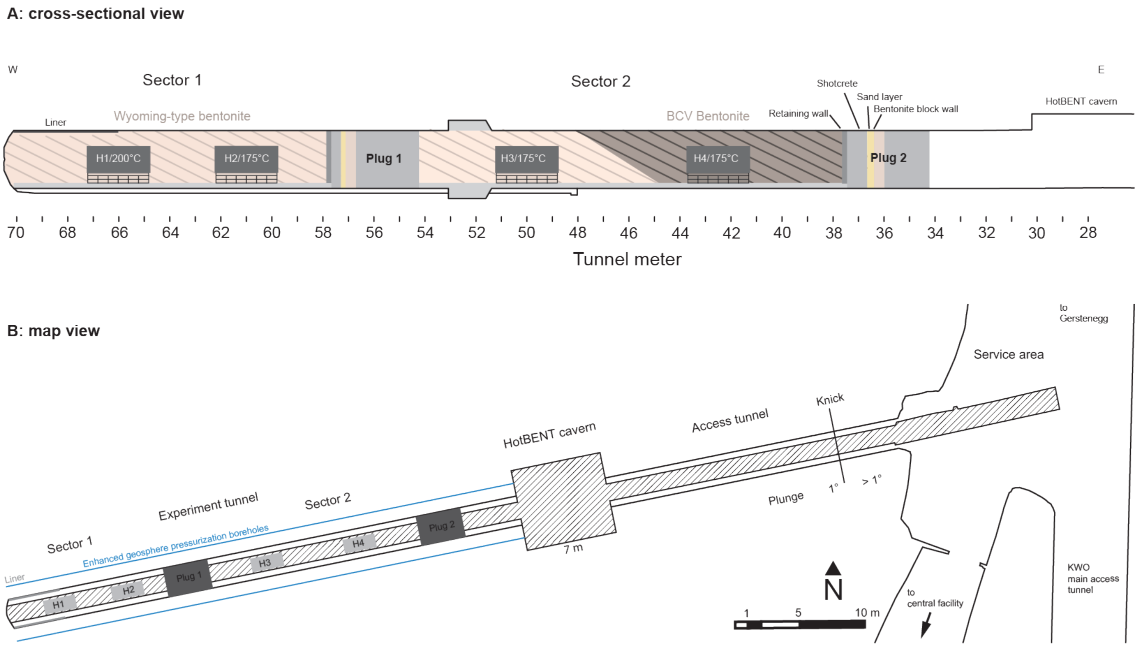

Fig. 1-1: Layout of HotBENT test (current design): A) vertical section, B) plan view showing HotBENT cavern

FEBEX in-situ test section from TM53 (plug) to tunnel end

1.2 Timeline of on-site activities and scope of the report

The on-site implementation of HotBENT was carried out between 2nd February 2020 and 9th September 2021, equivalent to a total of 344 working days (Fig. 1-2).

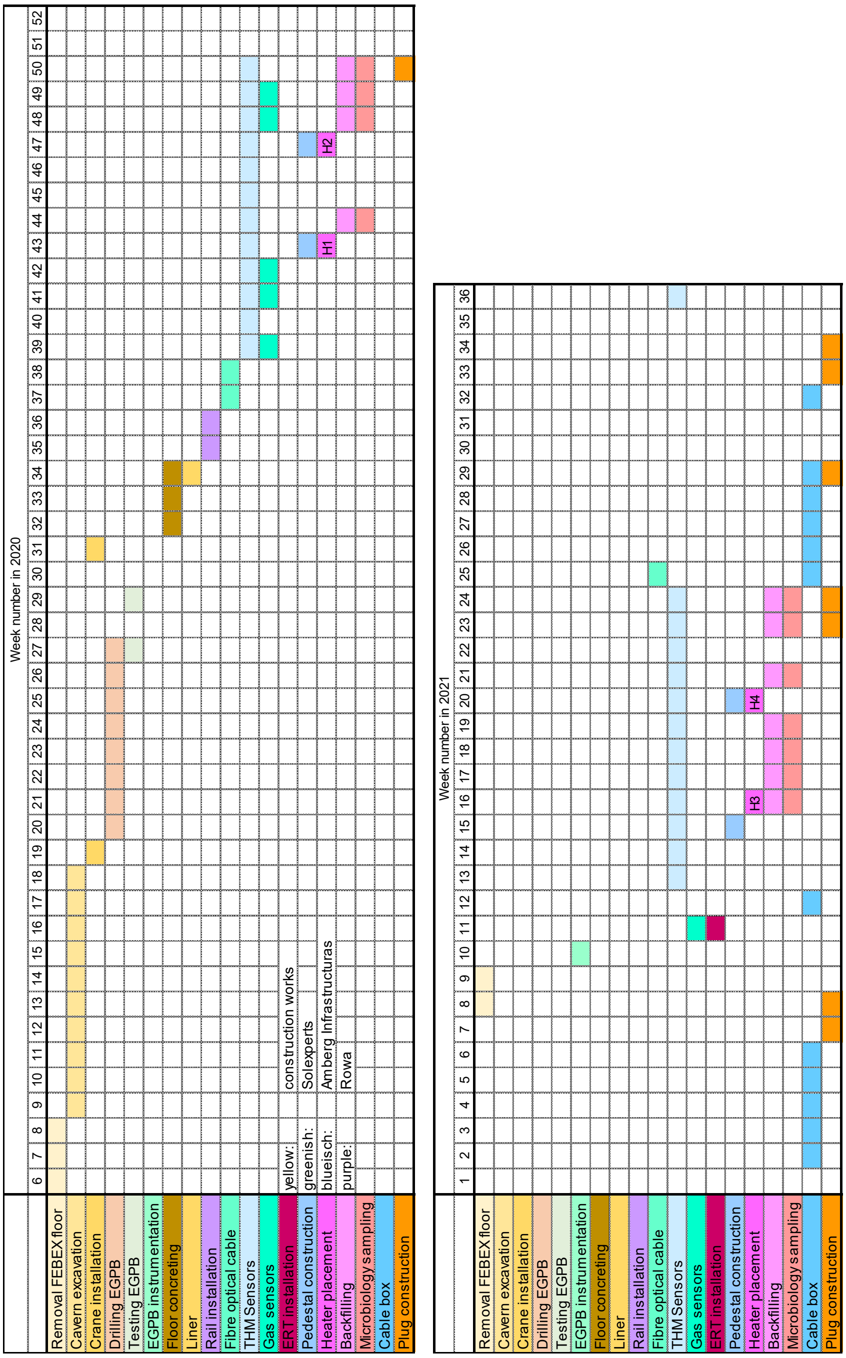

Fig. 1-2: Overall timeline for the on-site implementation of HotBENT

FEBEX: Full-scale Engineered Barrier System Experiment, EGPB: enhanced geosphere pressurisation boreholes, THM: thermo-hydro-mechanical; ERT: electrical resistivity tomography.

1.3 History of the HotBENT experiment and scope of this report

The first phase of on-site construction was dedicated to gallery preparatory work and is documented in Schneeberger et al. (2021). Following this, the installation work (sensor installation, heater emplacement, backfilling) started on 14th September 2020, with the installation of the fibre optic cable for distributed temperature sensing and thermal conductivity measurement. The installation of the four modules with approximately 1500 sensors was completed with the installation of displacement sensors on the front of Plug 2 on 9th September 2021. The entire installation of the instrumentation is documented in Kober et al. (in prep). The construction of the two sandwich plugs[1] and all other components manufactured with cementitious materials are reported in detail in Schneeberger and Kober (2022). Kober et al. (in prep.) will summarise the entire installation work in an as-built report. Heating started in parallel on 9th September 2021 for all four modules.

This report is dedicated to the components manufactured from bentonite, i.e. bentonite blocks and GBM. Chapter 2 focuses on the employed raw material. Chapter 3 is dedicated to the bentonite blocks. Chapter 4 describes the manufacturing of the GBM. The emplacement of the different bentonite materials in described in Chapter 5. Chapter 6 consists of the baseline characterisation of the various bentonite materials. Chapter 7 concludes the report.

---

[1] Sandwich plug: the plugs are constructed of several layers in a sandwich-like arrangement consisting of a retaining wall, two shotcrete layers, a sand layer and a bentonite block wall. The rationale of the sandwich plug is to decrease gas and water permeability while maintaining the mechanical confinement.

2 Raw bentonite materials

2.1 Introduction

Bentonite is a natural clay consisting mainly of smectite group minerals formed by low-temperature alteration of igneous deposits, typically volcanic ash deposits laid down in shallow marine environments (Grim and Güven 1978).

2.2 Requirements

Based on the experience from multiple precursor experiments (mainly FE, and HE-E) the following requirements were formulated for the HotBENT raw material (Tab. 2-1). It is important to note that two different types of bentonites were used in the HotBENT experiment. Bentonite around Heater Modules 1, 2 and 3 is an Na-dominated Wyoming-type bentonite, whereas Heater Module 4 was surrounded by Bentonite Černý Vrch (BCV) (Fig. 1-1). As the experience with BCV raw material for industrial-scale manufacturing of buffer materials (GBM and blocks) is limited, the requirements were solely formulated for the Wyoming-type bentonite and used as guidelines for the BCV heater module.

Tab. 2-1: Raw material requirements for the Wyoming-type bentonite (Garitte et al. 2015)

Criterion	**Requirement**
Material	Natural (non-activated) sodium bentonite
Smectite content by dried weight	> 75%
Additives (such as magnetite, baryte, binders or others)	No additives allowed
Cation exchange capacity (CEC)	> 70 meq/ 100g
Pyrite content by dried weight	< 1%
Sulphur content by dried weight	< 0.5% (corresponds to approx. 1% pyrite)
Organic carbon by dried weight	< 1%
Na_2O content by XRF	> 2 mass%
Grain-size distribution of the raw material	Well distributed between very fine and max. 1 mm (see Fig. 2-1).

2.3 Bentonite materials used for HotBENT

As mentioned before, two different types of bentonites were used during the HotBENT experiment (Chapter 1). The majority of the experiment (Heater Modules 1, 2 and 3) were backfilled with an Na-dominated bentonite stemming from Wyoming, whereas Heater Module 4 was backfilled (GBM and blocks) with BCV bentonite.

2.3.1 Na-dominated Wyoming-type bentonite (National® WP1000)

For Heater Modules 1, 2 and 3, both the bentonite blocks and the GBM were manufactured from an Na-dominated Wyoming-type bentonite. The selected bentonite was purchased from CEBO Holland B.V., Ijmuiden, Netherlands under the trade name National® WP 1000 for the GBM and

National® 1802 for the blocks. The two bentonites stem from the same crude but vary in grain-size distribution. National® WP1000 is characterised by an even grain-size distribution between 0 and 1 mm, whereas National® 1802 is characterised by an even distribution between 0.2 and 1.8 mm.

The following characteristics were indicated by the raw material supplier (Tab. 2-2).

Tab. 2-2: Characteristics of National® 1802 as indicated by the supplier

Parameter	**Test method / in accordance with**	**Typical property**
Moisture content	DIN 1812-1	12%
Enslin value after 24 hours	DIN 18132	850%
Filtrate water loss	ASTM D5891	15 ml
Swell index	ASTM D5890	30 ml
Smectite /montmorillonite	XRD	82 mass%
Na-feldspar	XRD	3 mass%
K-feldspar	XRD	0 mass%
Quartz	XRD	2 mass%
Calcite	XRD	0
Trydymite	XRD	0
Cristobalite	XRD	5
Illite	XRD	3
Clinoptilolite	XRD	2
Heulandite	XRD	3

The Enslin value is indicative of free water absorption (Kiviranta and Kumpulainen 2011, Kaufhold et al. 2010)

Furthermore, the raw material National® WP1000 is characterised by a grain-size distribution as shown in Fig. 2-1. The grain-size distribution is well-sorted between 0 and 1 mm.

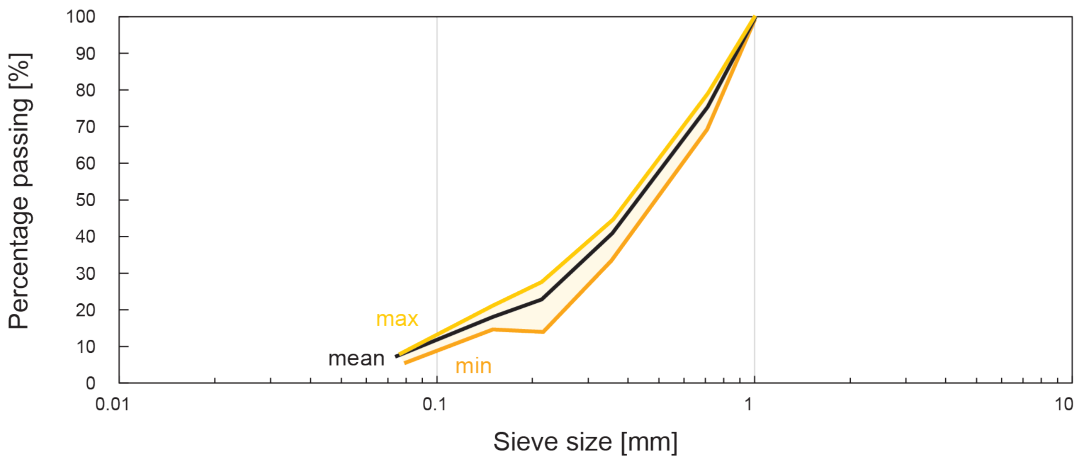

Fig. 2-1: Grain-size distribution of the raw material National® WP1000

2.3.2 Bentonite Černý Vrch (BCV)

Heater Module 4 was placed on BCV blocks and backfilled with BCV GBM. The grain size of the raw material for the BCV GBM was between 0 and 1 mm and for the blocks between 0.6 and 2 mm.

BCV is a Ca-Mg-dominated bentonite purchased from the company Keramost (Hausmannová et al. 2018, Tab. 2-3). The initial moisture content was indicated as 6% for both the GBM and the blocks (personal communication Keramost).

Tab. 2-3: Characteristics of BCV as indicated by SURAO (Hausmannová et al 2018)

Parameter	**Test method / in accordance with**	**Typical property**
SiO_2	Silicate analysis	49.75 mass%
Fe_2O_3	Silicate analysis	11.11 mass%
Al_2O_3	Silicate analysis	14.8 mass%
MgO	Silicate analysis	2.5 mass%
Na_2O	Silicate analysis	0.34 mass%
CaO	Silicate analysis	3.1 mass%
TiO_2	Silicate analysis	3.04 mass%
K_2O	Silicate analysis	1.15 mass%
Calculated LOI	Silicate analysis	10.85 mass%
Smectite /montmorillonite	XRD	87 mass%
Quartz	XRD	8.5 mass%
Calcite	XRD	2 mass%
Kaolinite	XRD	1.5 mass%

3 Bentonite blocks

3.1 Introduction

In the experiment design of HotBENT (Garcia-Siñeriz and Tuñon 2020), bentonite blocks were used for two purposes. (a) compacted bentonite blocks were used as pedestals for the heater to ensure a centralised position of the heater and a safe working environment after emplacement of the heater and before backfilling with GBM. (b) a bentonite block wall was part of the sandwich plug to ensure relatively low permeability of the plug (Schneeberger and Kober 2022).

3.2 Design requirements

Two different bentonite types were used to compact bentonite blocks (National® 1802 for the bentonite block pedestals under Heaters 1, 2, and 3; and BCV for Heater 4). The compaction procedure was carried out in line with Garitte et al. (2015).

Two different shapes of bentonite blocks were required for the construction of the bentonite block pedestals, ordinary blocks and top blocks (Fig. 3-1). The dimensions of the blocks are of utmost importance to ensure a stable pedestal hosting the heaters, as the pedestals were constructed of stacked layers of blocks.

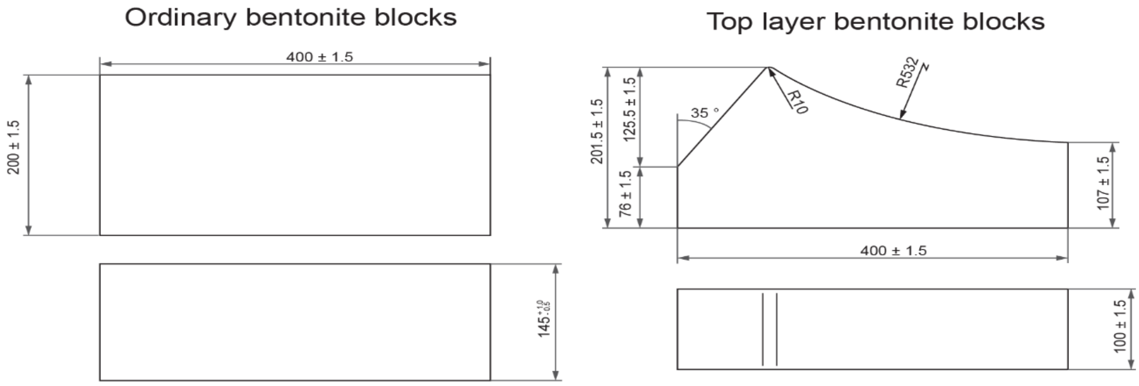

Fig. 3-1: Shapes of bentonite block required for the bentonite block pedestals

In addition to the shape requirements, further requirements were formulated based on the experience gained during the FE experiment (Garitte et al. 2015, Müller et al. 2017)

- The blocks have to be homogeneous on a macroscopic level
- The blocks are manufactured by uniaxial compression
- The targeted bulk wet density of the blocks must be greater than 2.0 g/cm^3. The associated compaction pressure will be around 130 MPa for the National® 1802 blocks and 80 MPa for the BCV blocks
- The blocks must have a minimum uniaxial compressive strength of 6 MPa
- The blocks must be free of large cracks (see detailed description further below)
- The bentonite must never be exposed to temperatures above 80°C
- The blocks must be protected against high or low relative humidity

3.3 Pre-production test for BCV ordinary blocks

3.3.1 Manufacturing

Based on the experienced gained during the FE experiment, it was decided that for the National® 1802 no pre-tests were required before production. However, the pressing of blocks from the BCV was never performed on an industrial scale and thus pre-tests were run in January 2020. During the testing of the compaction, 21 ordinary blocks of BCV were pressed. Based on initial tests, it was decided to increase the water content in the raw material of the BCV to 24 mass% compared to the originally used 19 mass%. The 19 mass% were used in analogy to the water content used in FE (Garitte et al. 2015).

The pressed blocks were manufactured with a compaction pressure of 80 MPa and yielded a uniaxial compressive strength of 15 MPa.

3.3.2 Quality control

The blocks were measured and weighed at Haasser Ets facility in Soufflenheim, France (Tab. 3-1). The geometric quality control confirmed the compliance of the blocks to the targeted characteristics as defined in Section 3.2.

Tab. 3-1: Geometric quality control on the pre-production blocks at the factory

Block number	Length	Width	Height	Volume	Weight	Wet density
	[mm]	[mm]	[mm]	[cm^3]	[g]	[g/cm^3]
1	399.6	200.7	145.6	11677.08	24300	2.08
2	399.7	200.8	145.7	11693.85	24300	2.08
3	399.6	201.2	145.2	11674.01	24320	2.08
4	399.8	201.4	145.2	11691.46	24360	2.08
5	399.7	200.8	145.2	11653.72	24300	2.09
6	399.7	200.8	145.6	11685.82	24300	2.08
7	399.7	200.5	145.7	11676.38	24260	2.08
8	400	200.5	145.8	11693.16	24440	2.09
9	400	199.9	145.7	11650.17	24360	2.09
10	400	200.1	145.7	11661.83	24380	2.09
11	399.7	200.1	145	11597.1	24200	2.09
12	399.7	199.5	145.6	11610.17	24140	2.08
13	399.7	199.8	145.8	11643.6	24160	2.07
14	399.7	200.3	145.7	11664.73	24160	2.07
15	399.7	199.6	145.6	11615.99	24120	2.08
16	399.7	199.6	145.6	11615.99	24120	2.08
17	399.6	199.5	145.6	11607.26	24120	2.08
18	399.8	199.6	145.7	11626.87	24100	2.07
19	399.9	200.2	145.5	11648.73	24160	2.07
20	399.7	199.7	145.6	11621.81	24120	2.08
21	399.7	199.5	145.6	11610.17	24100	2.08

Upon delivery of the blocks at GTS, a simple loading test was performed. The loading experiment consisted of loading two blocks stacked upon each other with a weight similar to the heater. Cameras recorded the evolution of the blocks under load at relative humidity conditions of the GTS. The loading experiment was carried out in two different locations at GTS with different ambient relative humidity conditions. The ventilation cavern (VE) is characterised by a relative humidity in the air of approximately 60 to 70%. Conditions are wetter in the Bohrkranz cavern (BK) with relative humidity values of around 80% (Fig. 3-2).

The BCV blocks were stable until the loading test ended after approximately seven months of loading. In a first phase, desiccation cracks were observed in the blocks in the VE cavern, but with increasing ambient relative humidity, the cracks healed[2]. No cracks were observed in the blocks loaded in the BK cavern.

[2] Ambient relative humidity at GTS is subject to annual fluctuation (Schneeberger et al. 2019)

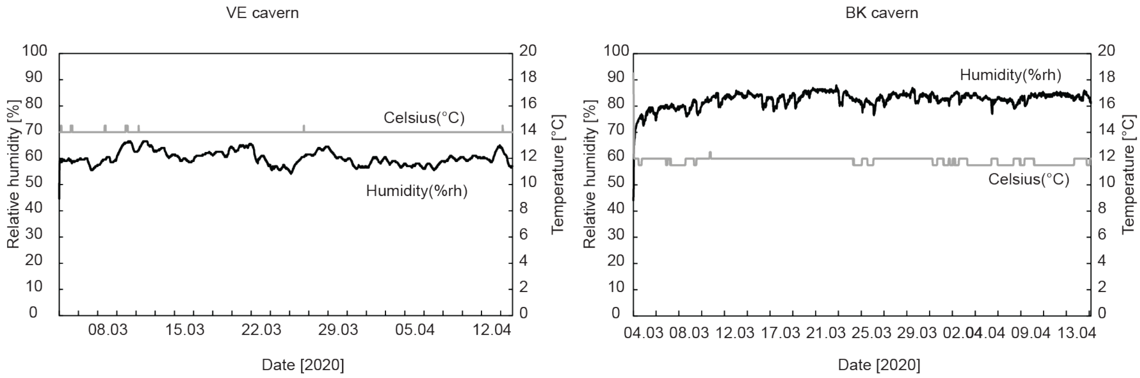

Fig. 3-2: Relative humidity evolution in the VE cavern and the BK cavern over 1 month

In addition to the loading experiment, the equilibrium relative humidity of the BCV block was determined. The equilibrium relative humidity is the ambient air relative humidity at which the moisture content in the air and in the bentonite block is in equilibrium. This means that moisture is neither added nor subtracted from the bentonite block. Within the FE experiment, an empirical thumb-rule was established, indicating that if the ambient relative humidity is within a range of ±10 percent points of the equilibrium relative humidity of the blocks, the blocks will remain stable. Beyond that range, blocks might either swell or dry and thus lose strength with time.

The equilibrium relative humidity for the BCV blocks was around 81% (Fig. 3-3). It is important to note that the equilibrium relative humidity is dependent on the water content of the blocks, which, in turn, is dependent on the water content of the raw material.

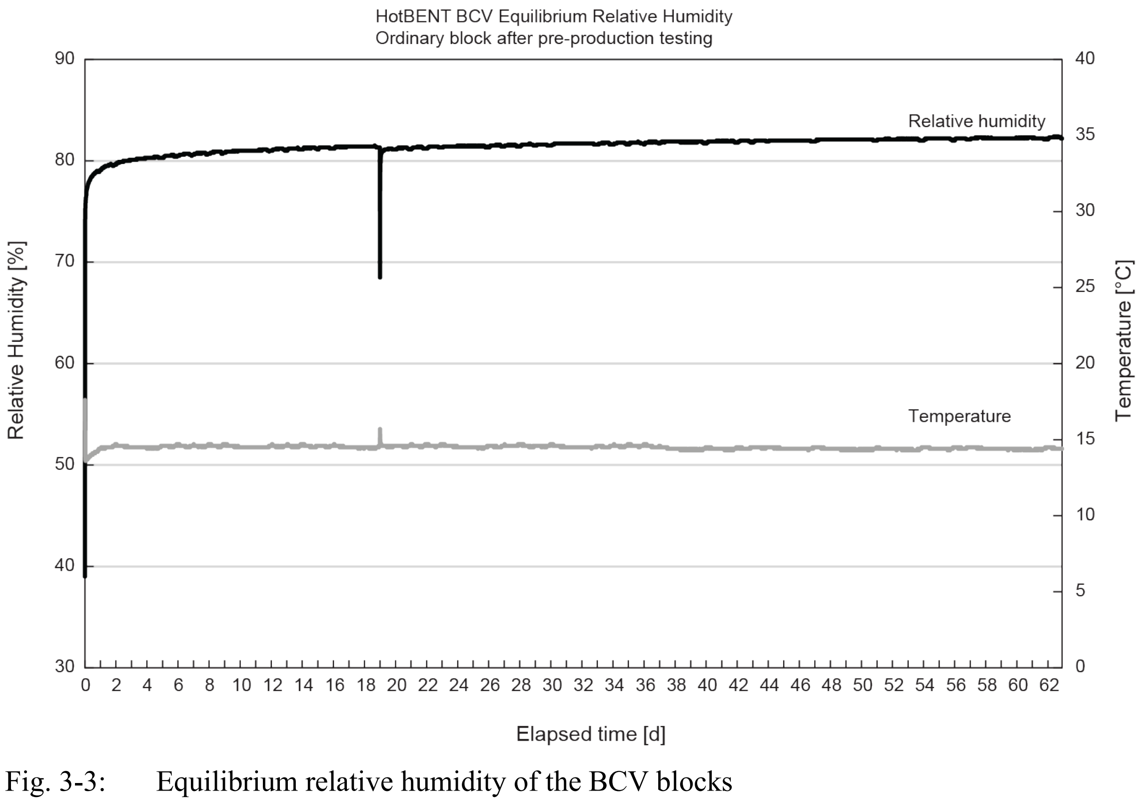

Fig. 3-3: Equilibrium relative humidity of the BCV blocks

Upon arrival of the blocks at GTS, water content measurements were performed. Five samples from different locations on two blocks were taken for the measurements (Tab. 3-2). Water content in the BCV blocks was decreased compared to the water content of the raw material (24 mass%). The blocks were characterised by a water content in the range between 20.1 and 20.5 mass% (mean of the five samples: 20.3). The decrease in water content of the bentonite blocks compared to the raw material is likely related to moisture loss during pressing of the blocks.

Tab. 3-2: Water content measurements on pre-production BCV ordinary blocks at GTS

Bentonite type	Sample ID	Relative position in block	Wet sample mass	Dry sample mass	Water mass	Water content
			[g]	[g]	[g]	
BCV	05//20-1	Top	92.49	76.949	15.541	0.202
BCV	05//20-2	Bottom	91.42	75.969	15.451	0.203
BCV	05//20-3	Centre	93.23	77.388	15.842	0.205
BCV	05//19-1	Top	88.31	73.557	14.753	0.201
BCV	05//19-2	Bottom	83.93	69.759	14.171	0.203

3.4 Block production for HotBENT

Based on the pre-production tests carried out for the BCV blocks and on the experience from FE (Garitte et al. 2015), the block production for HotBENT was launched.

3.4.1 Water content adjustments

Water content adjustment to the raw materials for the block production (National® 1802 and BCV) were carried out with tap water in Livorno, Italy. The water content of the National® 1802 was increased to between 18.1 and 20.4 mass% (mean: 19.3 mass%) and to between 24.2 and 25.5 mass% for the BCV (mean: 24.9 mass%).

During the manufacturing of the BCV ordinary blocks, it was observed that the blocks stuck to the mould very strongly. The ordinary blocks could not be pressed, and thus a second batch of BCV ordinary blocks was pressed with a water content in the raw material of approximately 19 mass%.

3.4.2 Manufacturing

Manufacturing of the blocks started with the National® 1802 blocks and ended with the pressing of the BCV ordinary blocks. The pressing was performed on the LAEIS 1600 Press (Fig. 3-4) at the facilities of Haasser Ets in Soufflenheim, France.

Fig. 3-4: Impressions from the bentonite block manufacturing

From left to right: LAEIS press, conveyor belt with pressed blocks, BCV blocks, National ® 1802 blocks

During the manufacturing of the BCV ordinary blocks, it was observed that blocks were sticking to the moulds so that it was not possible to obtain intact blocks. Therefore, a second pressing campaign was carried out for the BCV ordinary blocks with a lower water content in the raw material. The second pressing was successful.

After pressing, the blocks were packed carefully for the transport to GTS to ensure no damages to the blocks during transportation either due to mechanical impacts or water ingress. The packaging was performed according to the experience gained in FE (Garitte et al. 2015). The typical block packaging consisted of a wooden pallet, a paper sheet, layers of Styrofoam in between each layer of blocks and multiple plastic foils wrapped around the entire pallet to ensure water tightness.

3.4.3 Quality control and characterisation of the blocks

3.4.3.1 At the factory

During production, three different quality controls were carried out at the factory. Each block was inspected for cracks and was weighed. The weight test was used as indication for the dry density. Blocks failing the weight test or the crack quality control were discarded.

A definition of crack dimensions that would have led to a rejection of a block is shown in Fig. 3-5.

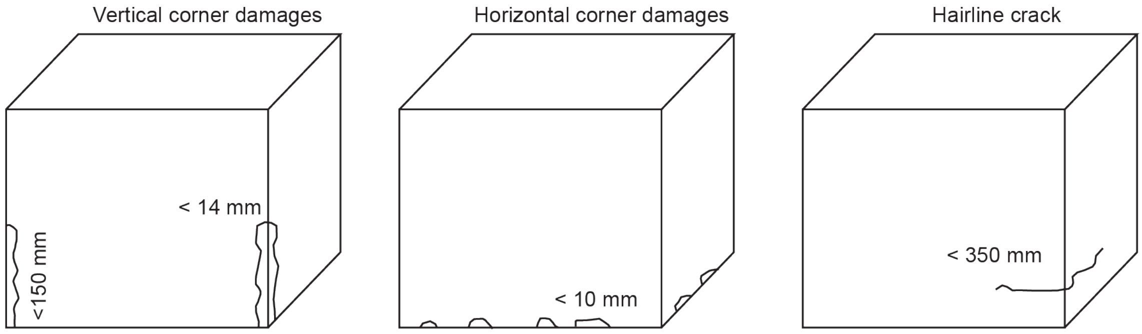

Fig. 3-5: Allowed maximum damages in the blocks after production

In addition to the weight test and crack control, the dimensions of 11 blocks were measured during the production of the ordinary blocks of National® 1802 (Tab. 3-3). During the production of the National ® 1802 top blocks, three blocks were quality controlled (Tab. 3-4). Unfortunately, no quality control was carried out at the factory during the production of the BCV blocks.

Tab. 3-3: Quality control on National® 1802 ordinary blocks at the factory

Ordinary Blocks - Bentonite Wyoming					
n° bloc	**Length**	**Width**	**Height**	**Mass [kg]**	**Wet density**
Requirement	400 ± 1.5	200 ± 1.5	145 +1/-0.5		2.08 ± 0.1
Units	[mm]	[mm]	[mm]	[kg]	[g/cm^3]
02/10	400	198.5	145.5	23.70	2.05
03/20	400	200	145.5	23.94	2.06
04/30	400	200	145.1	23.84	2.05
05/40	400	199	145.1	23.68	2.05
07/10	400	201.5	145	24.02	2.06
08/20	400	200	146	23.72	2.03
09/30	400	199	145.5	23.93	2.07
10/40	400	198.5	145.4	23.60	2.04
12/10	400	200	145.6	23.86	2.05
13/20	400	198.8	145.8	23.78	2.05
14/20	400	199	145.3	23.72	2.05

Tab. 3-4: Quality control on National® 1802 top blocks at the factory

Top Blocks - Bentonite Wyoming					
n° block	Length	Width	Height	Mass	Density
Requirements	400 ± 1.5	107 ± 1.5	100 +1/-0.5		2.08 ± 0.1
Units	[mm]	[mm]	[mm]	[kg]	[g/cm^3]
18/50	401	107.5	100	11.5	2.07
19/28	401	107.5	100	11.46	2.06
20/06	401	108	100	11.46	2.06

The uniaxial compressive strength was characterised for one ordinary block and one top block from National® 1802, respectively, and for one BCV top block (Tab. 3-5). Uniaxial compressive strength values for the National® are above the required threshold of 6 MPa. The values for the BCV blocks are below the value obtained during the pre-test, but only top blocks were tested during the main production, and the pre-test was carried out on ordinary blocks, which could explain the difference. In general, no threshold for the BCV was fixed as no experience on pressing BCV blocks was available prior to the HotBENT experiment.

Tab. 3-5: Uniaxial compressive strength measured on the produced blocks at the factory

Bentonite	**Block shape**	**Zone**	**UCS [MPa]**
National® 1802	Ordinary block	Top of the block	9
National® 1802	Ordinary block	Bottom of the block	8.5
National® 1802	Top block	Top of the block	6.9
National® 1802	Top block	Bottom of the block	8.4
BCV	Top block	Top of the block	5.2
BCV	Top block	Bottom of the block	4.8

3.4.3.2 At GTS

After arrival of the blocks at GTS, the water content was determined on selected blocks (Tab. 3-6 and Fig. 3-6). The water content in the blocks was slightly lower than the water content in the raw material (19 mass%), which could be related to moisture loss during pressing of the blocks.

Tab. 3-6: Water content measurements on the bentonite blocks after delivery to the GTS

Sample ID	Bentonite	Block shape	Drying time	Water content
1.1	National® 1802	Top	24 hours	18.59 mass%
1.2	National® 1802	Top	24 hours	18.17 mass%
2.1	National® 1802	Top	24 hours	18.64 mass%
2.2	National® 1802	Top	24 hours	18.33 mass%
1.1	National® 1802	Top	8 days	18.72 mass%
1.2	National® 1802	Top	8 days	18.31 mass%
2.1	National® 1802	Top	8 days	18.83 mass%
2.2	National® 1802	Top	8 days	18.34 mass%
3.1	National® 1802	Ordinary	24 hours	15.52 mass%
3.2	National® 1802	Ordinary	24 hours	15.95 mass%
4.1	National® 1802	Ordinary	24 hours	15.81 mass%
4.2	National® 1802	Ordinary	24 hours	15.91 mass%
3.1	National® 1802	Ordinary	8 days	15.67 mass%
3.2	National® 1802	Ordinary	8 days	16.04 mass%
4.1	National® 1802	Ordinary	8 days	15.88 mass%
4.2	National® 1802	Ordinary	8 days	16.27 mass%
1.2	BCV	Top	24 hours	23.76 mass%
1.1	BCV	Top	24 hours	23.25 mass%
2.1	BCV	Top	24 hours	23.59 mass%
2.2	BCV	Top	24 hours	23.68 mass%
1.1	BCV	Ordinary	24 hours	16.95 mass%
1.2	BCV	Ordinary	24 hours	17.10 mass%
2.1	BCV	Ordinary	24 hours	17.28 mass%
2.2	BCV	Ordinary	24 hours	17.42 mass%

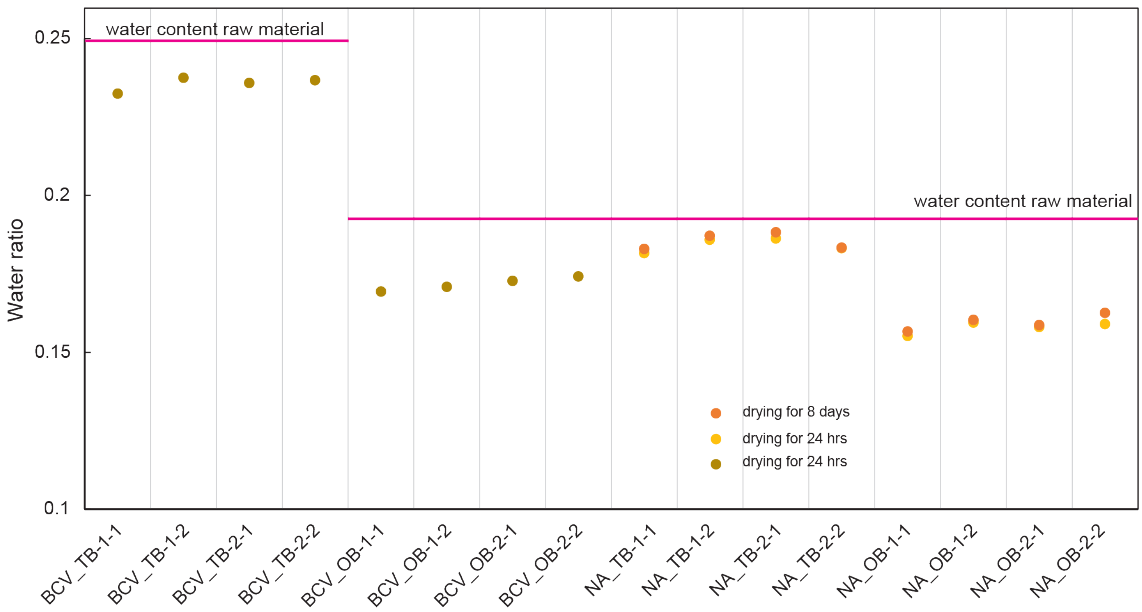

Fig. 3-6: Water content measurements in the bentonite blocks after delivery to the GTS

TB: Top block; OB: Ordinary block, BCV: Bentonite Černý Vrch, NA: National® Standard bentonite

In addition, equilibrium relative humidity measurements were carried out for the National® 1802 ordinary block and for the BCV ordinary block as the water content of the raw material had changed. The relative humidity for the National® 1802 ordinary block is around 71% and for the top block around 73%. The equilibrium relative humidity for the BCV ordinary block with a higher water content in the raw material is 67% and around 81% for the BCV top block. As mentioned above, the BCV top blocks were pressed with a higher water content in the raw material than the BCV ordinary blocks.

Based on the water content values reported in Tab. 3-6 and the volumes and masses of the blocks reported in Tab. 3-3 and Tab. 3-4, the dry density of the National® 1802 blocks was calculated (Tab. 3-7).

Tab. 3-7: Dry density values for bentonite blocks

Refer to Fig. 3-1 for the exact shape requirements on the blocks

Ordinary blocks – National® 1802						
Sample ID	Length	Width	Height	Mass	Density	Dry density
	[mm]	[mm]	[mm]	[kg]	[g/cm^3]	[g/cm^3]
02/10	400	198.5	145.5	23.70	2.05	1.77
03/20	400	200.0	145.5	23.94	2.06	1.78
04/30	400	200.0	145.1	23.84	2.05	1.77
05/40	400	199.0	145.1	23.68	2.05	1.77
07/10	400	201.5	145.0	24.02	2.06	1.78
08/20	400	200.0	146.0	23.72	2.03	1.75
09/30	400	199.0	145.5	23.93	2.07	1.79
10/40	400	198.5	145.4	23.60	2.04	1.76
12/10	400	200.0	145.6	23.86	2.05	1.77
13/20	400	198.8	145.8	23.78	2.05	1.77
14/20	400	199.0	145.3	23.72	2.05	1.77
Top blocks – National ® 1802						
18/50	401	107.5	100.0	11.5	2.07	1.75
19/28	401	107.5	100.0	11.5	2.06	1.74
20/06	401	108.0	100.0	11.5	2.06	1.74
Ordinary blocks – BCV						
1	402	202.1	146.7			
2	402	203.1	146.7			
3	402	202.2	146.9			
Top blocks - BCV						
	Length*	Vertical height*	Total height*	Width*		
Target**	400 ± 1.5	75 ± 1.5	201.5 ± 1.5	100 ± 1.5		
	[mm]	[mm]	[mm]	[mm]		
1	392	76.3	198.3	98.4		
2	393	74.2	197.0	98.6		
3	394	75.8	197.8	98.6		
4	396	76.3	198.3	99.0		
5	395	75.0	197.8	98.0		
6	393	74.3	195.5	98.0		
7	391	73.4	195.8	98.0		
8	395	75.1	198.3	100.5		
9	394	76.4	198.2	98.8		

* refer to Fig. 3-1 for details; ** formulated as target based on the requirements set for the National® 1802 top blocks

The average dry density of the National® 1802 ordinary blocks is 1.77 kg/dm^3 and 1.74 kg/dm^3 for the top blocks.

The dry density calculations for the BCV blocks rely on the average weights of the blocks used for the construction of the bentonite block pedestals. Thus, only one value for the ordinary blocks and one value for the top blocks is calculated. The volume of the BCV ordinary blocks is approximately 12 dm^3 and the average weight is 23.1 kg[3]. The average dry density is consequently 1.70 kg/dm^3. The average volume of the top blocks is 5.6 dm^3, and the average mass is 11.3 kg. Consequently, the average dry density of the BCV top blocks is 1.63 kg/dm^3. In general, the dry density values for the BCV blocks are lower than for the National® 1802 blocks, which might be related to the higher water content in the top blocks and the lower compaction energy used for the pressing of the ordinary blocks to prevent them from sticking to the mould.

[3] Weight of the BCV blocks was taken before emplacement in the bentonite block pedestal for Heater 4

4 Granular bentonite material (GBM)

A dry density of the GBM above 1.45 g/cm^3 after emplacement is targeted for the HotBENT project (Nagra 2019). The dry density of the GBM is used as proxy for the effective emplaced density of swelling smectite minerals which influences buffer parameters such as hydraulic conductivity or swelling capacity (Dixon et al. 2002).

4.1 Manufacturing and quality control

The manufacturing of GBM aims at maximising the dry density of the emplaced GBM while trying to keep the suggested procedure industrially feasible. It is commonly known that the dry density of the GBM increases if the dry density of the pellets increases and the inter-pellet porosity, being the porosity in between the pellets, decreases (Fig. 4-1). The target dry density of the GBM after emplacement is shown in grey.

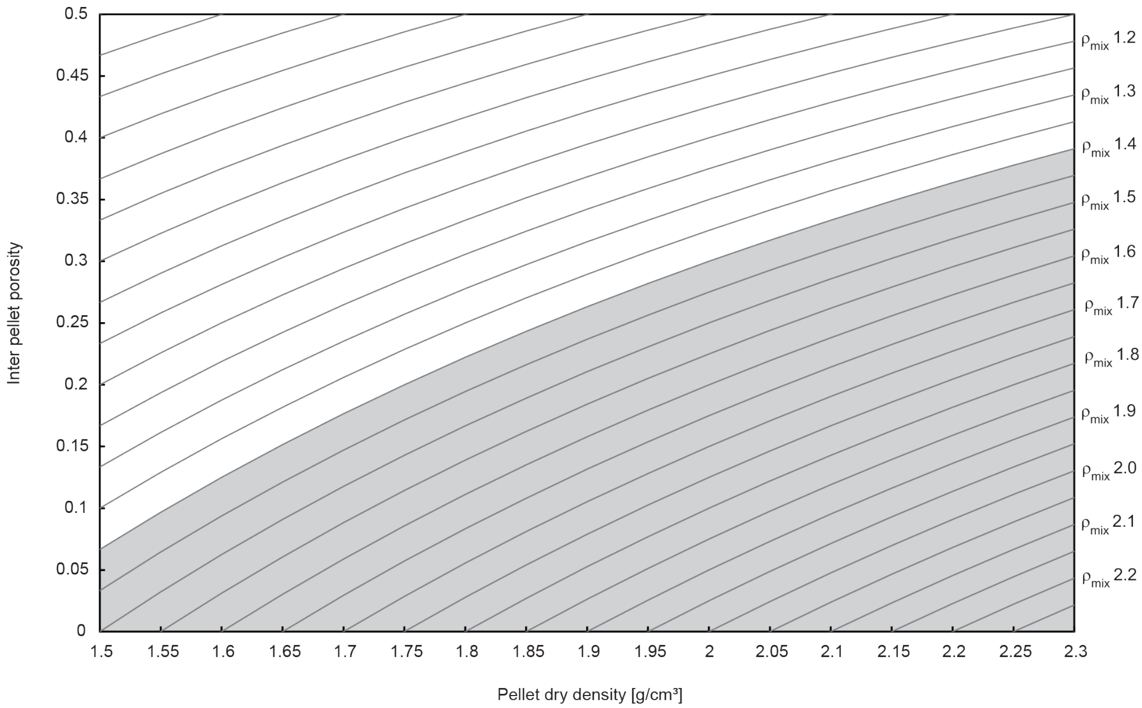

Fig. 4-1: Dry density of a pellet mixture as function of the pellet dry density and the inter-pellet porosity

From the dependency of the mixture density on the pellet dry density and the inter-pellet porosity, it follows that both the pellet dry density as well as the inter-pellet porosity have to be optimised to reach the target emplaced dry density. Among other factors, the pellet dry density depends on the grain-size distribution and the water content of the raw material but also on the compaction energy (Proctor 1933). The inter-pellet porosity is dependent on the grain-size distribution of the final GBM mixture and on the emplacement technique.

The manufacturing of the GBM in HotBENT was based on the experience gained during FE and reported in Garitte et al. (2015).

4.2 Pelletisation

It is commonly observed that the dry density of the pellets decreases with increasing water content in the raw material (Garitte et al. 2015). This is true for water contents on the "wet" side of the proctor curve, as the proctor curve describes the maximum dry density under a given compaction energy for a specific water content. Therefore, the water content (mass of water divided by mass of solids) was decreased for the National® WP1000 from initially 13.6 mass% to 6.5 mass%. The variability in water content of the raw material for National® WP1000 is shown in Fig. 4-2. No measurements on the raw material of the BCV were carried out. The supplier indicated a water content of 6.4 ± 1.5 mass% of the raw material.

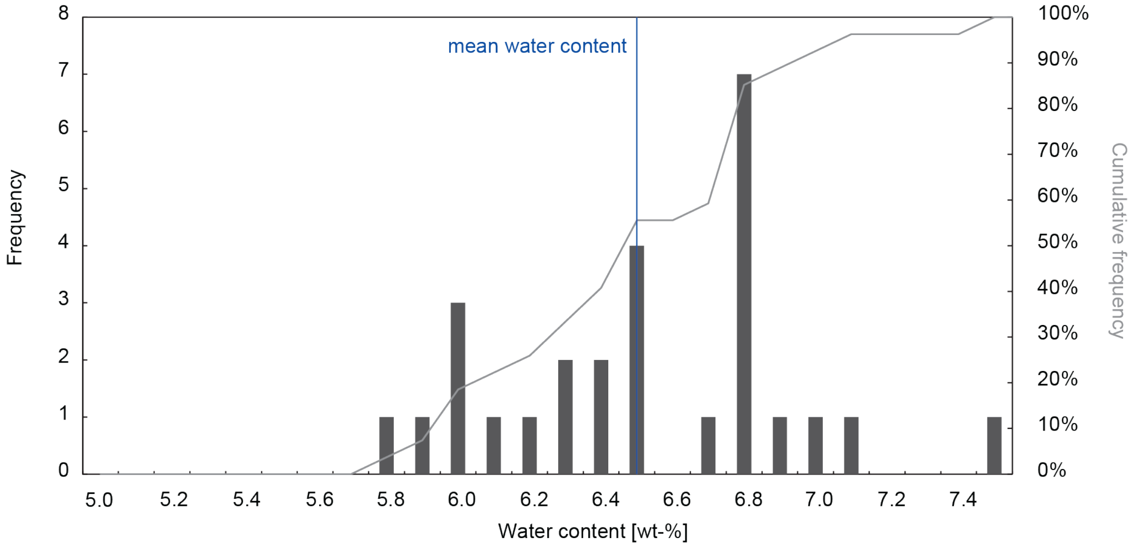

Fig. 4-2: Water content of National® WP1000 raw material used for GBM manufacturing

Water content of the raw material was decreased by CEBO Holland B.V. from an initial 12 mass% to the values presented in Fig. 4-2.

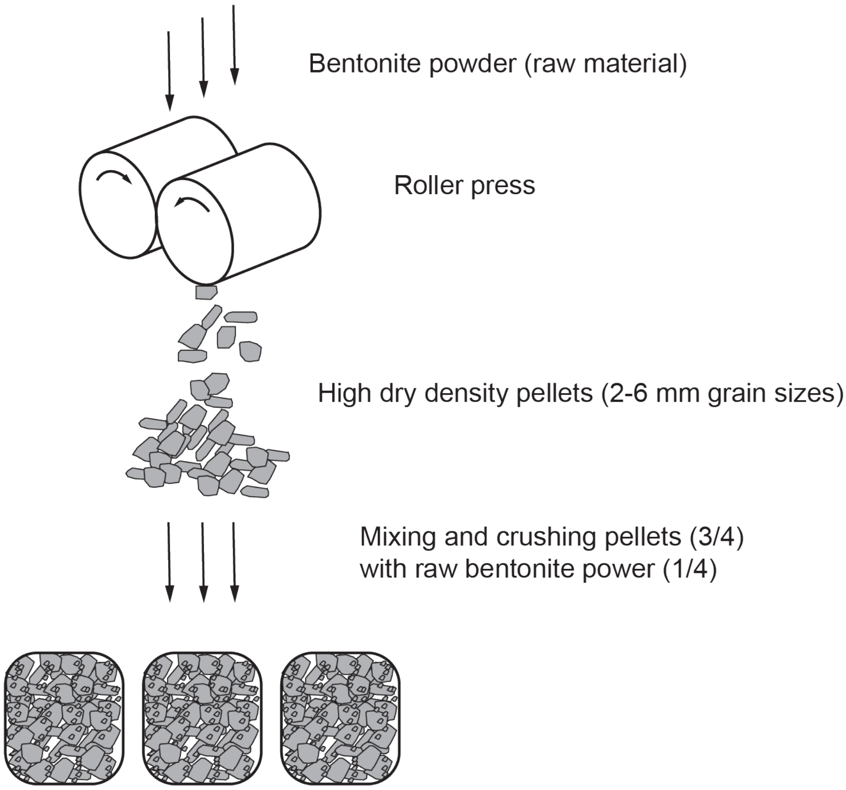

Fig. 4-3: Process of pelletisation (modified after Hofmann et al. 2007)

The manufacturing of the GBM was carried out by J. Rettenmaier & Söhne GmbH + Co KG, Rosenberg, Germany.

Three quarters of the total raw material were pelletised with large stainless-steel barrels (Fig. 4-3). The compaction by roller press resulted in highly compacted pellets with grain sizes between 2 and 6 mm (Fig. 4-4). No difference in the grain-size distribution was observed between the National® WP1000 pellets and the BCV pellets.

After the pellets were manufactured, their dry density was measured following the procedure described in Garitte et al. (2015), where a given weight of pellets is immersed in olive oil to measure the volume of the pellets, but to prevent them from swelling. The average dry density values for pellets from National® WP1000 and from BCV amount to 2.0 g/cm^3 (Fig. 4-4), with a larger spread in the dry density values obtained for the National® WP1000.

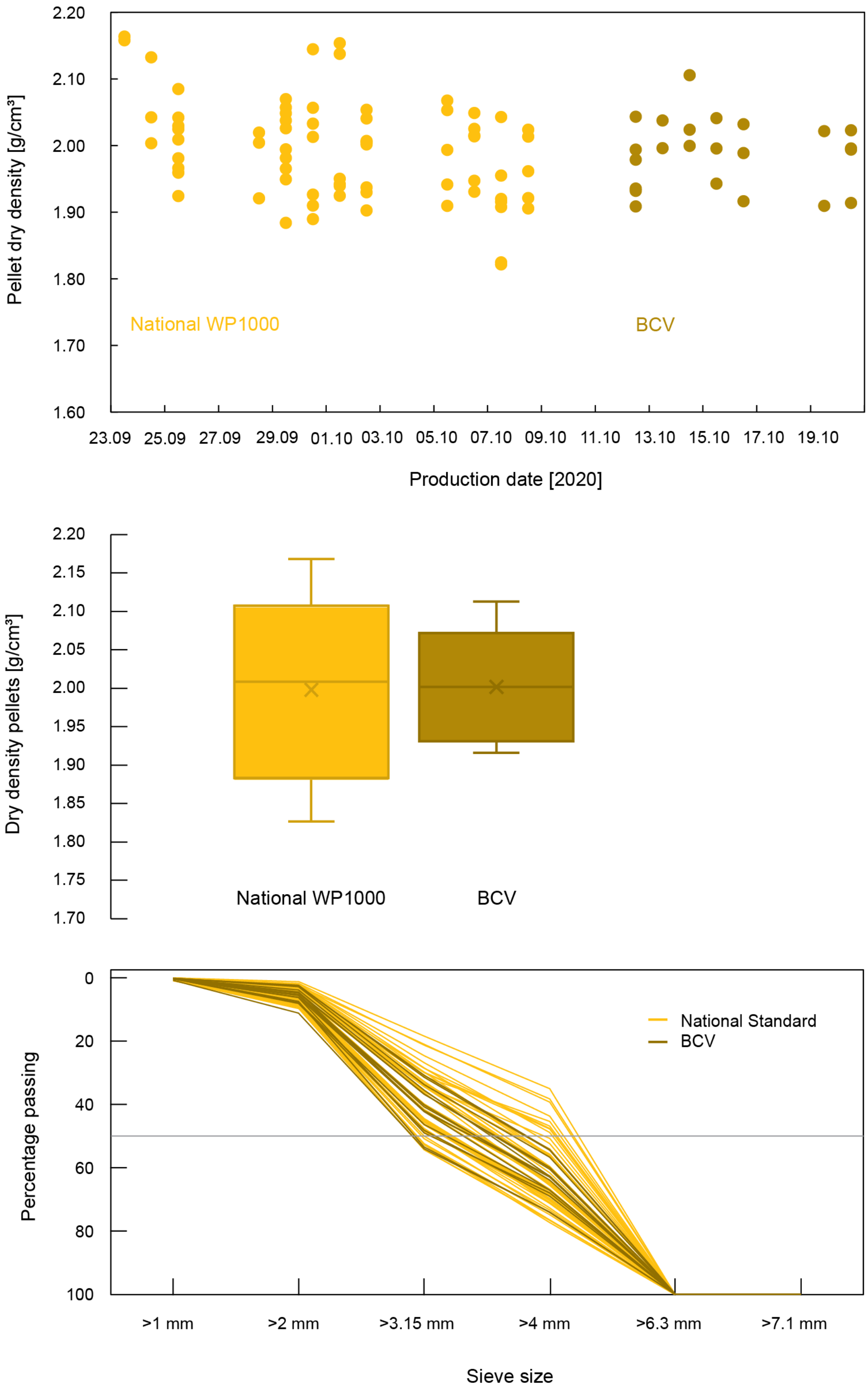

Fig. 4-4: Quality control after pelletisation

Top: Pellet dry density after pelletisation per production date; centre: box plots showing pellet dry density distribution; bottom: grain-size distribution of the pellets after production

Between 23rd September and 9th October, pellets were produced from National® WP1000, and from 12th October to 20th October, pellets were produced from BCV.

It was observed that the water content of the pellets had slightly decreased compared to the water content of the raw material. This reduction of water content is related to the compaction of the raw material to obtain the pellets, which generally leads to moisture loss.

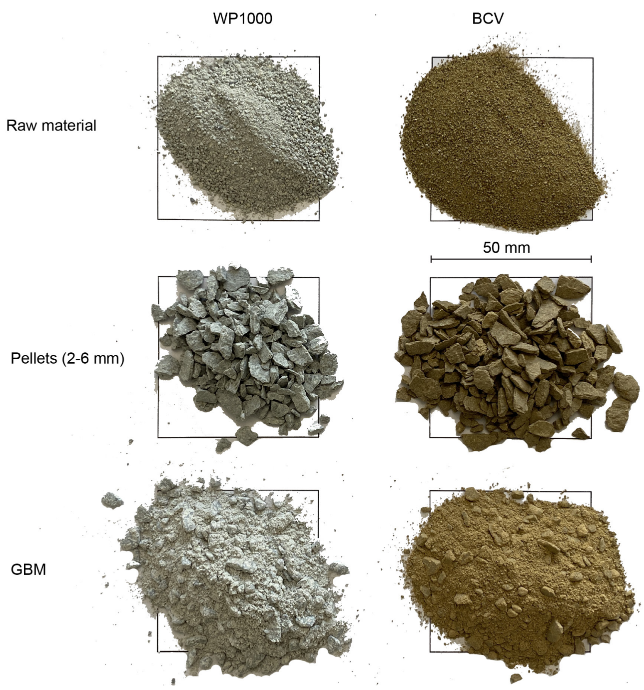

Fig. 4-5: Pictures of the different bentonite products during GBM manufacturing

4.3 Mixing and rounding

After production, the pellets were mixed with raw material for 30 min. at 2700 rpm (rounds per minute). The final mixture mass consists of ¾ pellets and ¼ raw material. Impressions of the final GBM for HotBENT are given in Fig. 4-5.

The loose density of the GBM was measured for each mixture (Fig. 4-6), whereby a grain size sieving curve was determined for every tenth mixture. Loose density is defined as gravitationally compacted density.

The average loose wet density is 1.46 ± 0.03 g/cm^3 (mean ± 2σ) for the National® WP1000 bentonite and 1.46 ± 0.02 g/cm^3 (mean ± 2σ) for the BCV bentonite. This has to be corrected for the water content. Thus, the dry loose density is approximately 1.37 g/cm^3 for the National® WP1000 and 1.37 g/cm^3 for the BCV (Fig. 4-6).

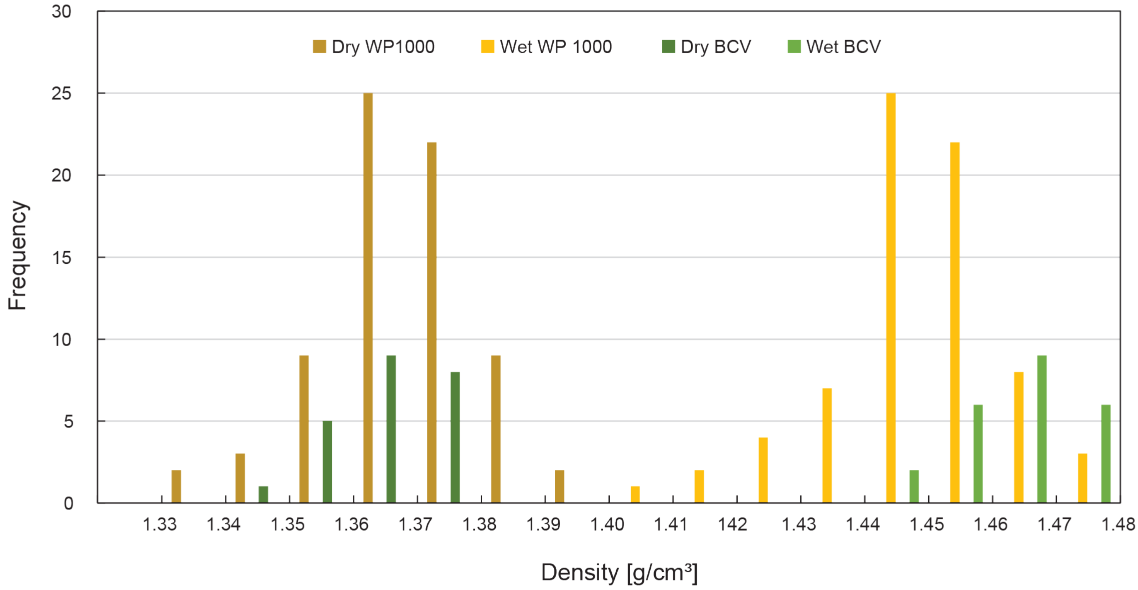

Fig. 4-6: Histogram showing loose density (dry and wet) for the National ® WP1000 and BCV GBM

During production of the GBM, a sieving curve analysis was performed for every tenth mixture. The sieving curve analysis was carried out with 500 g of material and three minutes of shaking with intervals. The resulting sieving curve is shown in Fig. 4-7. The Fuller curve (Fuller and Thompson 1907) describes the grain-size distribution for a given maximum grain size (Dmax) and a shape factor (n) for the particle that results in minimal inter-particle porosity and thus highest density. Compared to the Fuller curve, the GBM grain-size distribution is depleted in fine grains and shows slight enrichment in grains between 0.6 and 1 mm.

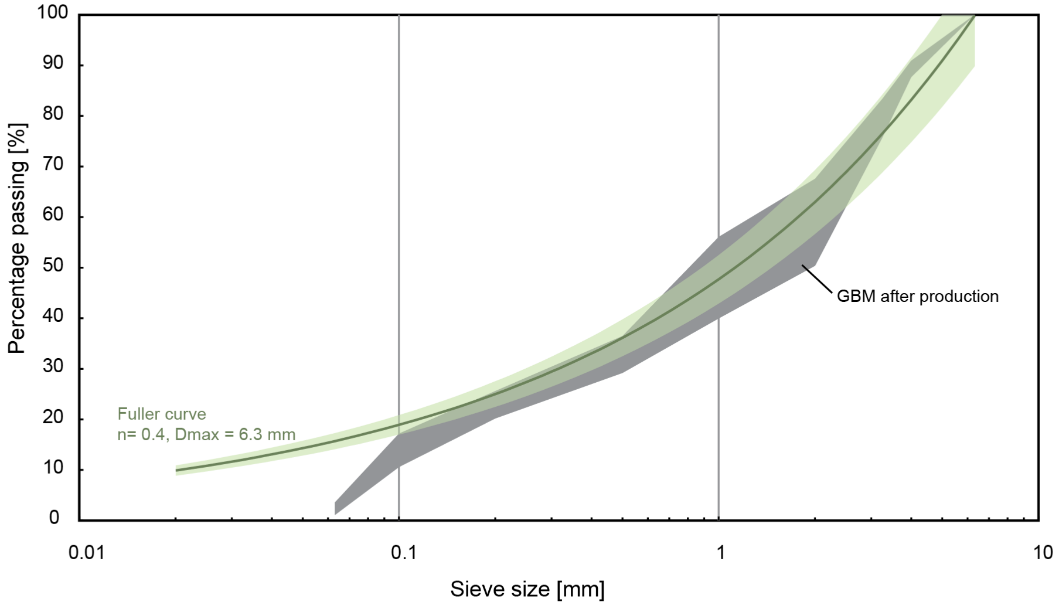

Fig. 4-7: Sieve curve analysis of GBM after production

Number of analyses: 8 for National® WP1000 GBM and 4 for BCV GBM

4.4 Packaging and transport

The final GBM was packed into 0.5 m^3 big bags. Commonly 1008 ± 9 kg (mean $\pm 1\sigma$) of GBM were filled into one big bag. Each big bag was placed on a paper sheet covering a wooden pallet. Each bag was covered with a rain plastic sheet and wrapped into plastic foil (Fig. 4-8).

Fig. 4-8: Impressions from the packaging of the GBM

Left: filling the GBM into big bags; right: packed big bag with relative humidity sensor (red arrow)

The multiple packaging was performed to avoid any water uptake of the GBM during transportation. The transport was carried out with lorries containing 22 GBM big bags each (Fig. 4-8). The GBM was delivered to the GTS between 29th September 2020 and 28th October 2020 to the GTS.

A relative humidity sensor was included to big bag number 1 for the National ® WP1000 to monitor the evolution of the surrounding relative humidity (Fig. 4-10). However, the relative humidity sensor was not placed into the bentonite (Fig. 4-8), but rather on the bag and thus monitored the ambient conditions surrounding the bentonite big bag.

Fig. 4-9: Transport of the GBM big bags to the Grimsel Test Site

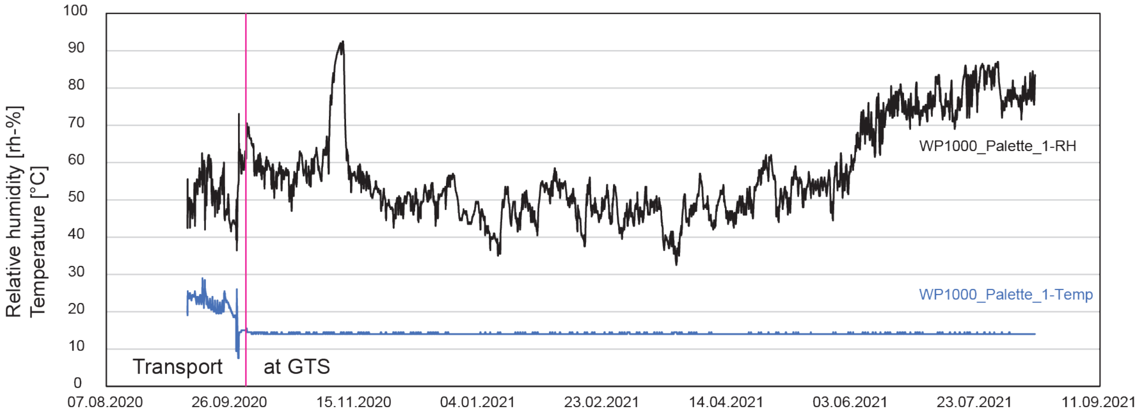

Fig. 4-10: Evolution of relative humidity and temperature in the vicinity of GBM big bag number 1 of National ® WP1000

Big bag #1 was never emplaced and is still at GTS

4.5 Quality control at GTS

The equilibrium relative humidity values for the GBM were measured in a manner similar to that for the bentonite blocks (Section 3.3.4.2, Fig. 4-11). The values are lower than for the blocks which correlates with the lower water contents of the raw material. The equilibrium relative humidity of the National® WP1000 GBM is around 35% and around 17% for the BCV GBM. A comparison of the equilibrium relative humidity values with the measured relative humidity values during the evolution of the experiment will be performed at a later stage.

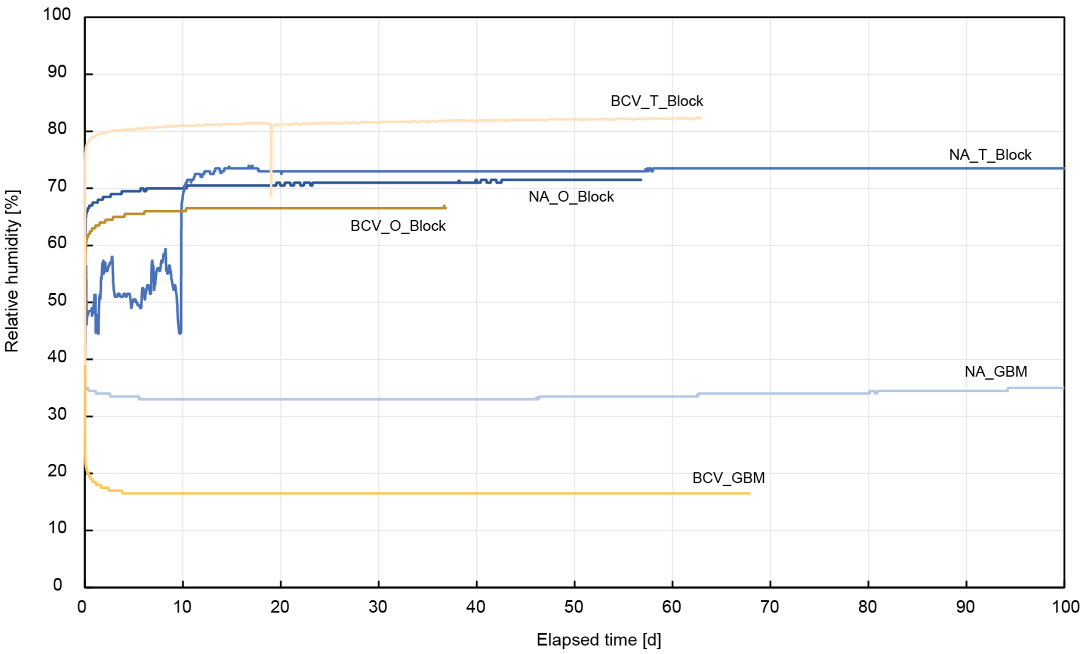

Fig. 4-11: Equilibrium relative humidity for the National® 1802 and BCV ordinary and top blocks and the GBM

BCV_T_Block: BCV top block, BCV_O_Block: BCV ordinary block, BCV_GBM: BCV granular bentonite material

NA_T_Block: National® 1802 top block, NA_O_Block: National® 1802 ordinary block, NA_GBM: National® WP1000 granular bentonite material

5 Emplacement in HotBENT

5.1 Emplacement of the bentonite blocks in HotBENT

Four bentonite block pedestals were constructed during the implementation of the HotBENT experiment to host the four heaters (Fig. 1-1). Three pedestals were constructed from National® 1802 bentonite blocks and one pedestal was constructed from BCV bentonite blocks. The blocks in all pedestals were laid out in a similar manner (Fig. 5-1 and Fig. 5-2). The block layout was designed to reduce the number of throughgoing block boundaries. The width of the block pedestal is 80 cm and the total length 240 cm. This is 10 cm shorter than the length of the heaters (250 cm) for the practical purpose of securing the heater with temporary steel rods during instrumentation.

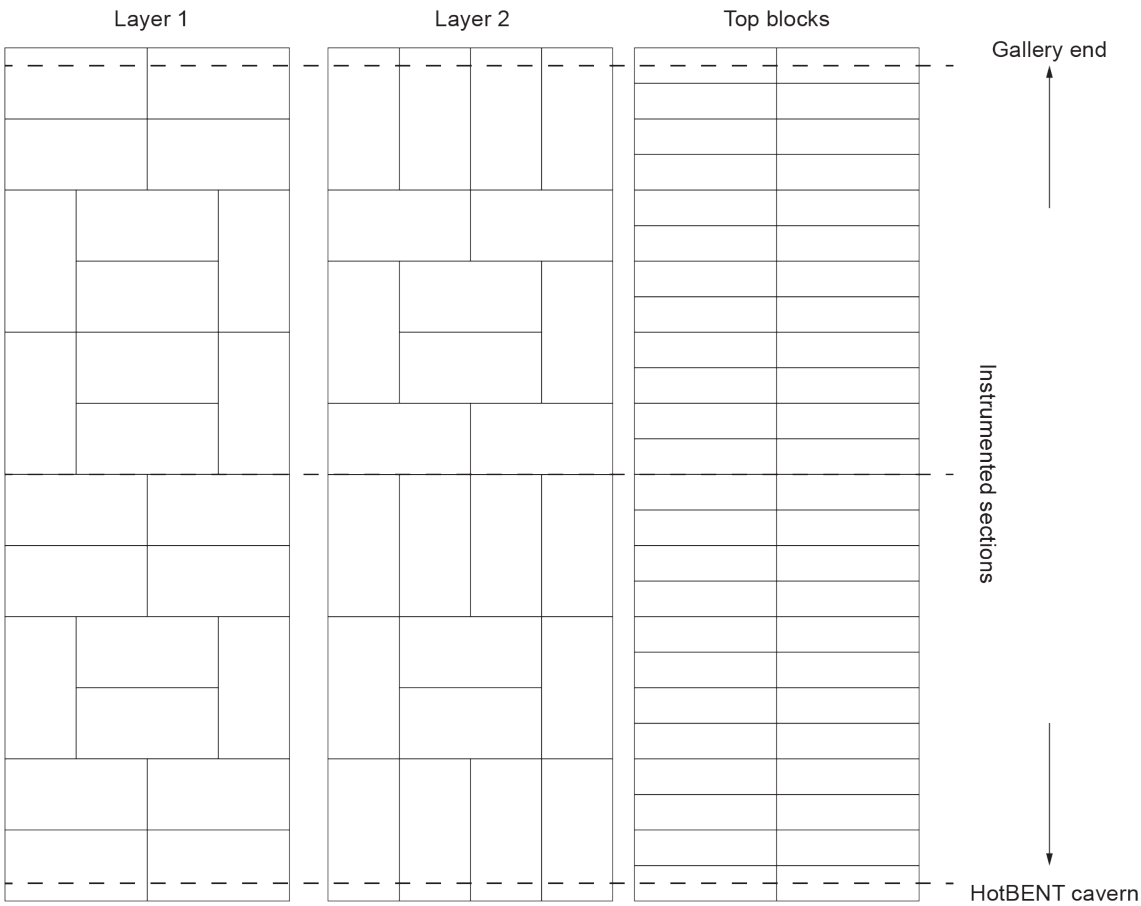

Fig. 5-1: Bentonite block arrangement in the heater pedestals

Layer 1 lies on the concrete invert and the top block layer is below the heater

Fig. 5-2: Impressions from the construction of the bentonite block pedestal

The two left pictures show National® 1802 bentonite blocks of Heater Pedestal 3. The two right pictures show BCV bentonite blocks of Heater Pedestal 4

Before erecting the pedestals, the blocks were incised to house sensors for recording temperature, pore pressure, relative humidity, total pressure and water content. The positions of the measurement section are indicated in Fig. 5-1. Details on the sensor layout inside the bentonite block pedestals are given in Kober et al. (in prep.). During the process of incising space for the sensors, each block was weighed before and after. In this manner, the exact weight of each pedestal was recorded. Before mechanisation, the average National® 1802 ordinary block weighed 23.7 kg, the BCV ordinary block 23.1 kg, the National ® 1802 top block 11.4 kg and the BCV top block 11.3 kg. The weight differences between the National ® 1802 and the BCV blocks are small. The differences might be related to different compaction pressures used during the pressing process.

Alterations to the blocks to accommodate the sensors resulted in a removal of 8.5 to 10.6 kg of bentonite. The weight of each heater pedestal is shown in Tab. 5-1. Based on the weight and the sum of the volumes of the bentonite blocks, the density and the dry density of the entire bentonite block pedestals were calculated. Note the volume of the pedestal is a minimum volume as it represents the sum of the individual volumes of the blocks. The real pedestal was slightly larger, but the true volume was not precisely recorded. The density and the dry density values for each pedestal can therefore be considered as best-case values.

Tab. 5-1: Weight of each heater bentonite block pedestal

	Units	Pedestal H1	Pedestal H2	Pedestal H3	Pedestal H4
Mass	[kg]	1670.9	1682.4	1679.6	1644.5
Volume*	[dm^3]	825.6	825.6	825.6	825.6
Density	[kg/dm^3]	2.02	2.04	2.03	1.99
Dry density	[kg/dm^3]	1.74	1.75	1.75	1.67

* The volume was estimated based on the sum of the volumes of the blocks assuming that no spaces are left between the individual blocks

H: heater

5.2 Emplacement of GBM in HotBENT

5.2.1 Backfilling unit and procedure

During the implementation of HotBENT at the Grimsel Test Site, the GBM was emplaced using a backfilling unit. The backfilling unit was developed within the FE experiment carried out in the Mont Terri Rock Laboratory (Nagra 2019, Jenni and Köhler 2015). The backfilling unit consists of the five-auger machine and the feeder wagon (Fig. 5-3). The feeder wagon serves to bring the bentonite big bags over the hopper of the five-auger machine, thereby "feeding" it with bentonite.

Within the frame of HotBENT, the five-auger machine was modified to fit the smaller gallery geometry at the FEBEX gallery compared to the FE gallery. The adaptations were minor and consisted mainly of lowering the entire machine to fit into a 2.28 m diameter gallery.

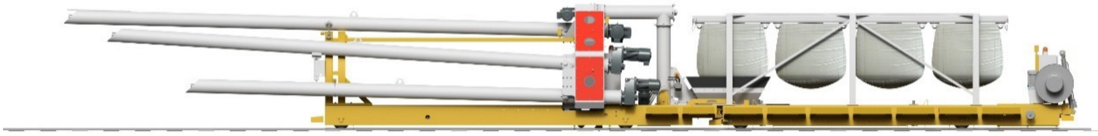

Fig. 5-3: Graphical visualisation of the backfilling unit with the five-auger machine in front and the feeder wagon with four bentonite big bags behind

Auger lengths between 7.86 m and 5.95 m, entire machine length: ~16 m

The backfilling sequence consisted of moving the five-auger machine forward, lifting the feeder wagon onto the rails, loading the feeder wagon with four GBM big bags, pairing the five-auger machine with the feeder wagon and finally backfilling. This sequence was reverted once backfilling had been completed. The feeder wagon was stored in the HotBENT cavern.

Impressions from the backfilling are shown in Fig. 5-4. Typically achieved backfilled slopes are shown in Fig. 5-5.

Fig. 5-4: Impressions from backfilling

Top left: five-auger machine from behind showing the hopper for the reception of GBM and its distribution to the five augers; top centre: five-auger machine from the front with the augers; top right: feeder wagon from behind showing the steering unit; bottom left: augers above the heater; bottom right: augers in the bentonite slope during emplacement.

Fig. 5-5: Typically backfilled slopes around the heater (left) and without the heater (right)

5.2.2 Emplacement slopes (ES)

After the completion of each backfilling step, the open surface of the bentonite forms a slope. This slope was surveyed using standard geodetic tools (Fig. 5-6).

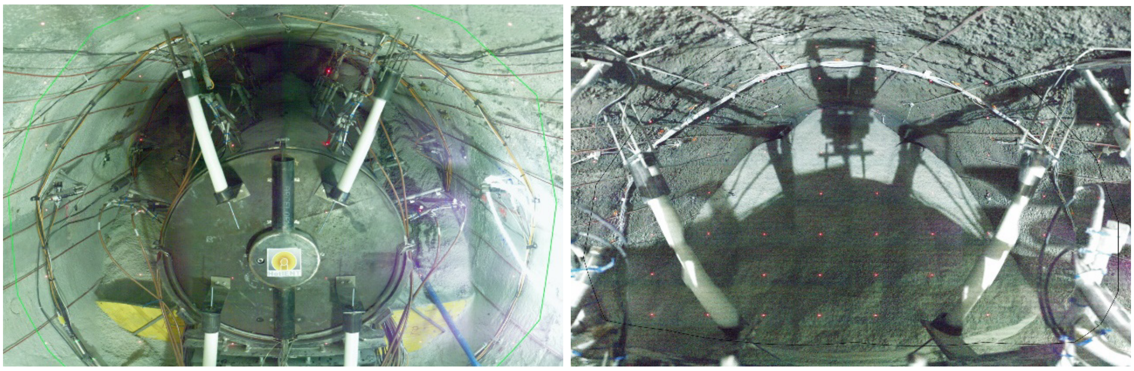

Fig. 5-6: Examples of emplacement slope surveying

Left: ES 5, Right: ES 21

The emplacement slopes are shown in Fig. 5-7. The bottom part of the slopes is usually vertical due to the usage of a temporary retaining wall to enable a longer backfilling section in the top part of the slopes while still allowing sufficient room at the floor to install the needed equipment or, for example, the bentonite pedestals (ES 31 in Fig. 5-7). Upon removal of the temporary retaining walls, the slope equilibrated slightly.

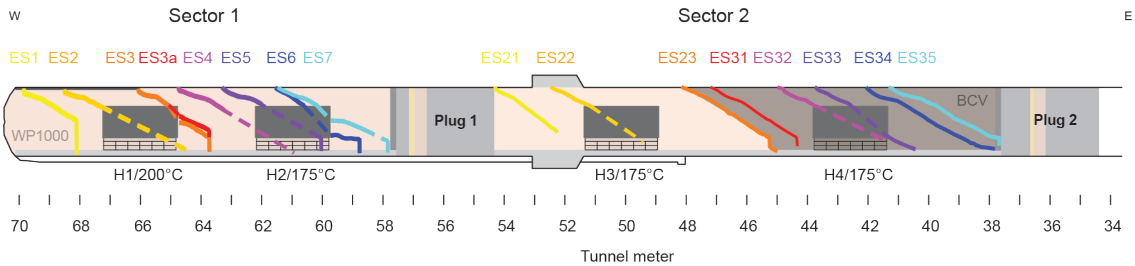

Fig. 5-7: GBM emplacement slopes along an axis-parallel cross-section

5.2.3 Backfilled volumes

The backfilled volume was measured based on surveying each emplacement slope with a laser scanner. The position and angle of the slope were then integrated into the 3D model based on the scan of the empty tunnel (Schneeberger et al. 2021). The difference between the start and the end slope of each backfilling step amounts to the backfilled volume. The backfilled volumes per emplacement step are given in Tab. 5-2.

The backfilled volumes were corrected for the volumes of the heaters and the pedestals, but not for the volumes of the sensors and the sensor cables. Correction of the backfilled volume for the sensors and sensors cables would slightly increase the backfilled density values for the GBM, which would result in a marginal increase (around 0.01 g/cm^3).

5.2.4 Backfilled mass of GBM

The total mass of emplaced bentonite amounts to 61 tonnes for Sector 1 (backfilled solely with National® WP1000) and 86 tonnes for Sector 2 (National ® WP1000 and BCV) or a total of roughly 147 tonnes of GBM. Details on the volume per emplacement step and the backfilled mass of GBM are given in Tab. 5-2. The mass was calculated from the weight of the big bags prior to and after each backfilling step.

5.2.5 Backfilled GBM density

Based on the scanned volume of each emplacement step and on the measured mass of emplaced GBM, the backfilled GBM density was calculated (Tab. 5-2).

In general, it can be noted that the backfilled density of the first and the last emplacement step (ES1, ES 7, ES 21, ES 31, and ES 35) per sector are lower due to the fact that GBM was poured in and could not be properly stuffed using the augers. Further, the density of ES 33 appears comparatively low, which could be related to several issues with the backfilling unit during the last backfilling. This was attributed to wear on the machine and expressed as breaking of the augers or non-functioning of the motors. Most issues could be fixed on site, but the last backfilling steps were carried out with only four augers as the left roof auger was defective. This led to adjustments in the backfilling procedure requiring a halt to the backfilling although the augers were not fully stuffing. The backfilled density values for the individual emplacement steps should be considered carefully and an averaging over larger volumes is recommended.

The individual emplacement density values for Sector 1 are range from 1.49 to 1.58 g/cm^3 and for Sector 2 from 1.48 to 1.54 g/cm^3 when excluding the steps at the beginning or end of a sector or those related to the change in bentonite type between ES 23 and ES 31.

It should be noted that the emplaced density has to be corrected for the water content to obtain the dry emplacement density (see Section 5.2.6).

Tab. 5-2: Backfilling steps with emplaced mass of GBM and backfilled volume

		Backfilled volume	Backfilled mass	Emplacement wet density
		[m³]	[kg]	[g/cm³]
ES 1	National ® WP1000	6.696	9,177	1.37
ES 2	National ® WP1000	5.243	8,132	1.55
ES 3	National ® WP1000	6.13	9,691	1.58
ES 4	National ® WP1000	6.898	10,520	1.53
ES 5	National ® WP1000	4.02	6,039	1.50
ES 6	National ® WP1000	4.054	6,037	1.49
ES 7	National ® WP1000	2.123	3,018	1.42
Sector 1	National ® WP1000	**40.971**	**61,551**	**1.50**
ES 21	National ® WP1000	5.813	8,096	1.39
ES 22	National ® WP1000	7.338	11,108	1.51
ES 23	National ® WP1000	15.65	23,228	1.48
ES 31	BCV	3.511	5,037	1.43
ES 32	BCV	7.139	11,009	1.54
ES 33	BCV	3.386	3,306	0.98
ES 34	BCV	7.193	11,024	1.53
ES 35	BCV	3.594	5,029	1.40
Sector 2	BCV + National® WP1000	**58.156**	**85,898**	**1.48**
Total HotBENT	BCV + National® WP1000	**99.127**	**147,449**	**1.49**

5.2.6 Water content of emplaced GBM

During backfilling, numerous samples of the GBM were taken directly from the big bags. These samples were used to measure the gravimetric water content. The water content was measured according to the procedure suggested by Kiviranta and Kumpulainen (2011). Thus, samples were dried for 24 hours at 105 °C. The water content was measured as the ratio between the water mass and the solid mass (Equation 1, ASTM D2216-19).

$$w_c = \frac{m_w}{m_s}, \text{ where } m_w = m_{wet\ sample} - m_{dry\ sample} \text{ and } m_s = m_{dry\ sample} \quad (1)$$

In order to analyse the influence of the drying time, additional samples were dried for longer time periods (up to 8 days or 192 hours) at 105 °C (Fig. 5-8).

The obtained water content values are shown in Fig. 5-8 and Tab. 5-3. In general, it is observed that the water content for the GBM made of National® WP1000 is lower compared to the BCV GBM. Furthermore, the water content of the WP1000 GBM is invariant with longer drying periods, which indicates that the entire free water evaporated after 24 hours. The slight increase in water content of the BCV GBM with drying time could indicate that the samples were not completed dried after the 24-hour drying period. The higher water content of the BCV is in contradiction to the water content measured for the pellets where similar values were obtained for both the WP1000 and the BCV, but the final mass of the GBM consists of ¼ raw material. The water content in the raw material in the BCV was higher than in the WP1000 and thus the final GBM is also characterised by slightly higher water content values.

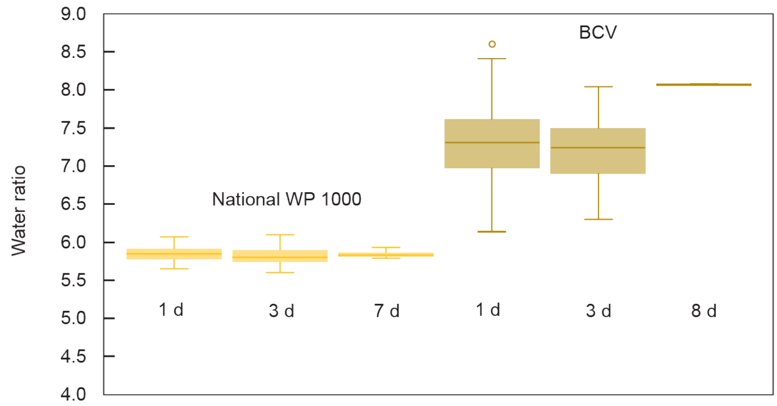

Fig. 5-8: Water content of emplaced GBM

Note the different drying times of 1, 3, 7 or 8 days

Tab. 5-3: Water content values for emplaced GBM

Bentonite type	Number of samples	Drying time	Average Wc	Standard deviation	Coefficient of variation
WP1000	34	24 hrs	5.85	0.10	0.02
WP1000	26	3 days	5.82	0.12	0.02
WP1000	8	7 days	5.85	0.05	0.01
BCV	26	24 hrs	7.27	0.58	0.08
BCV	22	3 days	7.22	0.44	0.06
BCV	4	8 days	8.07	0.01	0.001

5.2.7 Backfilled dry density of the GBM

Based on the obtained water contents, the emplacement densities obtained from the calculation of the mass of bentonite divided by the backfilled volume can be converted into emplacement dry densities. The dry density values are of interest as the density of swelling clay is of interest for the estimation of the swelling pressure.

The achieved emplacement dry density values are reported in Tab. 5-4. It is important to note that the calculation of the dry density per emplacement step assumes a homogeneous density within each backfilled step. Observations during the backfilling procedure indicate that the density within each backfilling step might be rather strongly heterogeneous with high-density areas around the augers and low-density areas behind the heaters.

Tab. 5-4: Emplacement dry density values for GBM per emplacement step and at selected intervals

	Backfilling volume	Bentonite mass	Water content	Dry density
	[m^3]	[kg]		[g/cm^3]
ES1	6.70	9177	0.058	1.30
ES2	5.24	8132	0.058	1.47
ES3	6.13	9691	0.058	1.49
ES4	6.90	10520	0.058	1.44
ES5	4.02	6039	0.058	1.42
ES6	4.05	6037	0.058	1.41
RW	7.93	11955	0.058	1.42
Sector 1	40.97	61551	0.058	1.42
H1	11.37	17823	0.058	1.48
H2	8.07	12076	0.058	1.41
H1-H2	26.35	40419	0.058	1.45
ES21	5.81	8096	0.058	1.32
ES22	7.34	11108	0.058	1.43
ES23	15.65	23228	0.058	1.40
Sector 2 Wyoming	28.80	42432	0.058	1.39
H3	22.99	34336	0.058	1.41
ES31	3.51	5037	0.072	1.34
ES32	7.14	11009	0.072	1.44
ES33	3.39	3306	0.072	0.91
ES34	7.19	11024	0.072	1.43
ES35	3.59	5029	0.072	1.31
RW	4.53	8061	0.072	1.66
Sector 2 BCV	29.36	43466	0.072	1.38
H4	17.72	25339	0.072	1.33

RW: retaining wall; H: heater

5.2.7.1 Backfilling procedure of GBM behind retaining wall

A special procedure was adopted for the backfilling behind the retaining wall, which formed the first element of the sandwich plug (further details on the sandwich plug are given in Schneeberger and Kober 2022). The retaining wall delimited the end of each sector, requiring the best-possible backfilling of the space behind it. Impressions from the procedure described in the following are given in Fig. 5-9. In order to achieve the highest-possible stuffing density of the GBM, construction of the retaining wall was segmented. The first element was installed, and backfilling was carried out with all five augers until the bottom of the emplacement slope reached the upper part of the first segment. Then the second element of the retaining wall was installed, and the lowest two augers were removed from the backfilling machine. The space behind the retaining wall was backfilled with the remaining three augers until the emplacement slope reached the upper part of the second element of the retaining wall. Lastly, only the top auger was used to backfill the space behind the third element of the retaining wall. The fourth and last element of the retaining wall was constructed with a square hole for the top auger. This procedure ensured that the highest-possible backfill density of the GBM behind the retaining wall. Additionally, man-made adjustments were made according to visual inspection, some shadow areas at the plug interface between the retaining wall and the bentonite had been insufficiently filled by the auger machine. Nevertheless, the backfilling density was not equal to the backfilling emplacement step without disturbing a retaining wall (Tab. 5-4). Hence, these emplacement steps should not be included in average backfill density estimates around the heaters.

Fig. 5-9: Impressions from the backfilling procedure behind the retaining wall

Top left: first element of the retaining wall and backfilling with five augers; top right: backfilling machine with only three augers; centre left: backfilling behind the second element of the retaining wall; centre right: auger machine with top auger; bottom left: square hole in fourth element of retaining wall; bottom centre: pushing GBM from the centre towards the side of the space behind the retaining wall to increase backfilling density; bottom right: retaining wall completed

5.2.8 General observations during backfilling

During the multiple backfilling steps, the following observations on the backfilling process were made.

- Backfilling density is suggested to be heterogeneous:
  - High dry density values in regions with proper auger coverage
  - Low dry density values behind heaters and central areas
  - Backfilling behind the retaining wall is hampered by the construction of the wall leading to lower dry density values close to the retaining wall
  - In Sector 2, cables were bundle on the tunnel roof leading to shadows and lower dry density values behind the cable bundle
  - At the beginning of each emplacement step, the augers had to be driven into the existing slope. Typically, the augers could no longer be inserted as deeply into the inserted slope after backfilling as had been possible before. The shallower position of the augers might influence the dry density of the start backfilling of each emplacement step
- Sliding and rolling of GBM on the emplacement slope results in a segregation of fine-grained material at the top and coarser-grained material at the bottom
- The backfilling machine could not always be supplied with GBM due to its inside the auger machine, occasionally allowing air to transported into the bentonite slope via the augers, resulting in small air escape (Fig. 5-10).

Fig. 5-10: Air escape during backfilling

6 Baseline characterisation

The aim of this chapter is to investigate and assess the compositional variation of both bentonites used in the entire experiment (homogeneity check) and to provide chemical reference data for the different materials used for HotBENT.

The differences between the bentonite materials used for GBM and blocks (National® Standard and BCV) were expected to be small. Chemical analysis using XRF and elemental C/S analysis (e.g. LECO oven) were selected for baseline characterisation because they provide accurate and reproducible values. Differences, if larger than analytical scattering, may reflect differences in phase contents which can be evaluated with XRD. XRD quantification, however, even in combination with Rietveld analysis, requires relatively large differences in phase contents and may be less suitable to detect minor differences. This technique is also time-consuming and requires expert knowledge.

At BGR, samples were analysed using standard analytical protocols. The GBM samples were investigated in LIMS (Laboratory Information Management System) order 52048 and the blocks samples were investigated in LIMS orders 52166 and 52277.

A complete list of the analysed samples is given in Appendix A.

6.1 Sample preparation

6.1.1 GBM samples

Three different types of GBM samples were analysed (National Standard® GBM used in HotBENT, National® GBM shipped to NWMO and BCV GBM used in HotBENT). The National® GBM samples used in HotBENT are labelled "NAS", the National® GBM samples shipped to NWMO are labelled "KAN", and the BCV GBM samples from HotBENT are labelled "BCV".

All samples reached BGR in sealed plastic bags. 10 g aliquots were taken as received from the bags which contained about 100 g sample mass each. Samples were ground by a rotary disc mill.

6.1.2 Block samples

The centre of each block was sampled using a 2 cm diameter steel drill (Fig. 6-1). Splitting was performed by a riffle splitter. Material from the uppermost part was not considered. Only material from the center of the blocks was used. Overall, each sample amounted to around 3 g. This material was dried at 60 °C (including determination of water content) and finally ground the same way as the GBM samples.

Fig. 6-1: Photographs of all blocks sent to BGR (left) as well as sampling of each block (right)

6.2 Chemical analyses (XRF + LECO) of GBM samples

The average loss-on-ignition (LOI) content of the samples BCV1-BCV23 was 17.0 mass%. Two samples showed elevated LOI contents (Fig. 6-2) which can either be explained by larger water contents in the precursor material or by water uptake during transport or laboratory treatment. The LOI content of the other bentonites was relatively constant. The LOI was determined by measuring the weight loss after heating to 1030 °C. All XRF values presented in the following were corrected according to the LOI (i.e. normalised to LOI = 0).

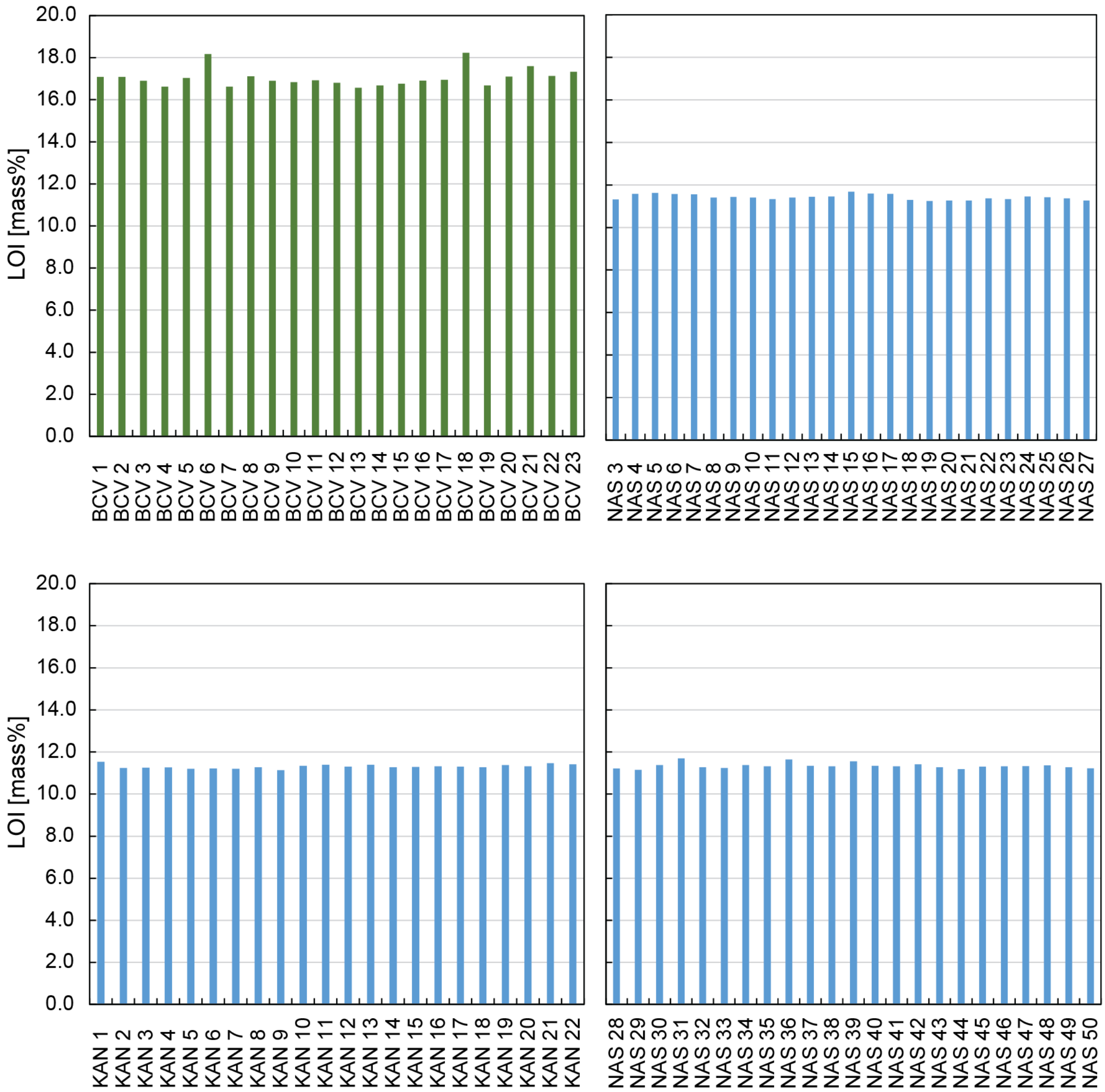

Fig. 6-2: LOI values of all GBM samples

The LOI of both the NAS sample series and the KAN sample series was 11.3 mass% on average.

In the following, selected element/oxide contents of all samples are compared (Fig. 6-3, Fig. 6-4, Fig. 6-5, Fig. 6-6, Fig. 6-7, and Fig. 6-8).

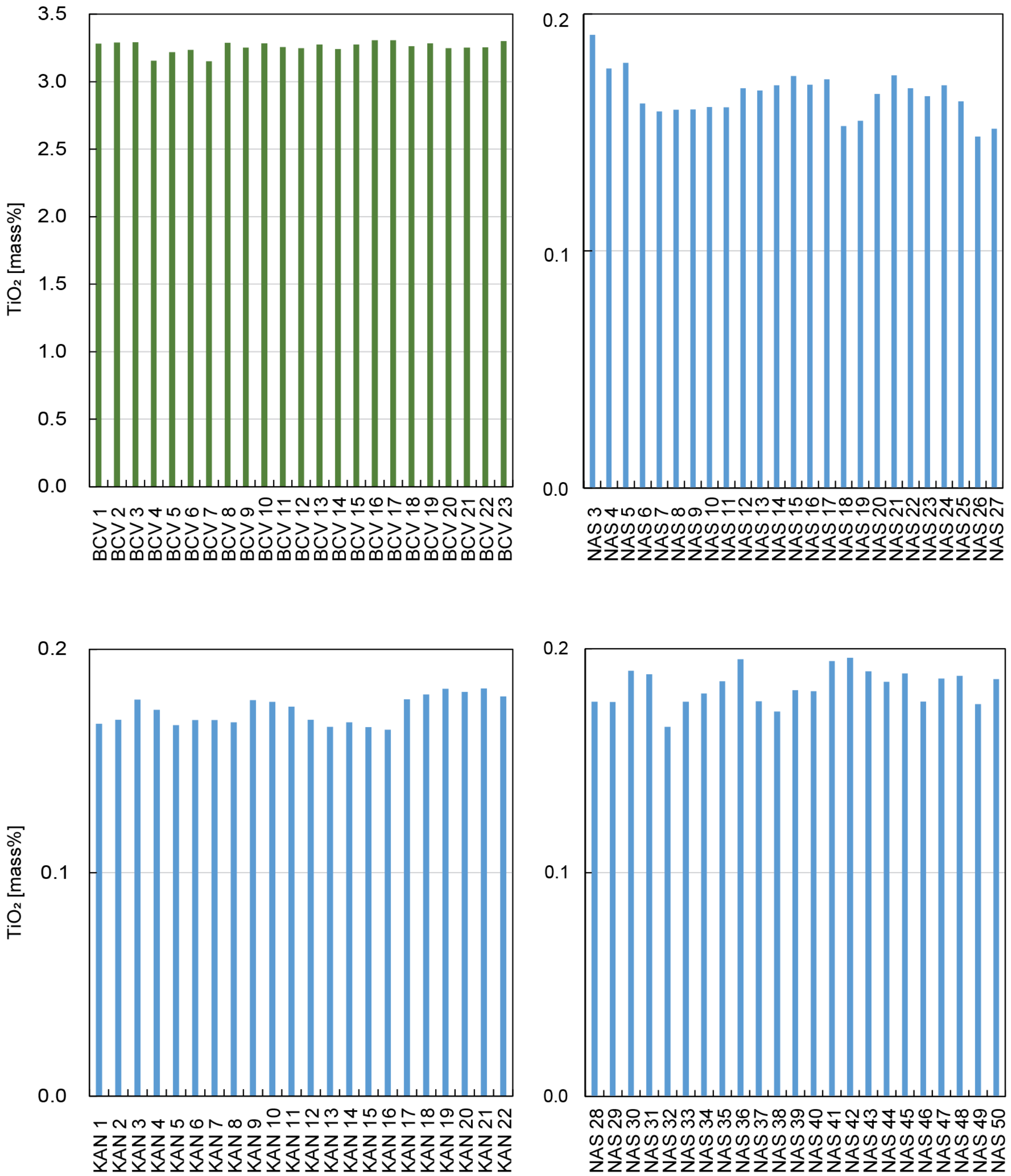

Fig. 6-3: TiO_2 contents of all GBM samples

Note differences in scales between BCV and National Standard® samples

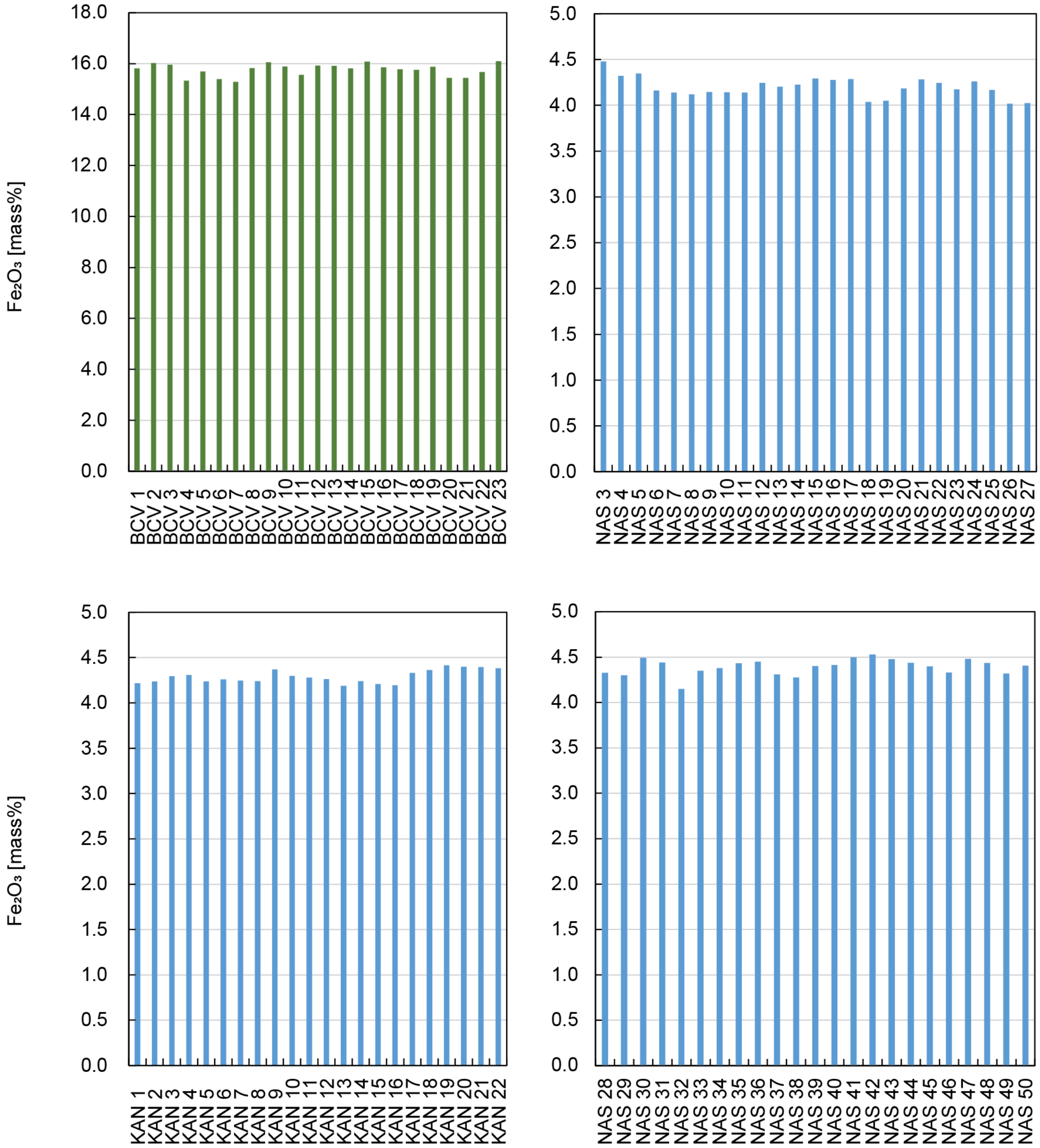

Fig. 6-4: Fe_2O_3 contents of all GBM samples

Note differences in scales between BCV and National Standard® samples

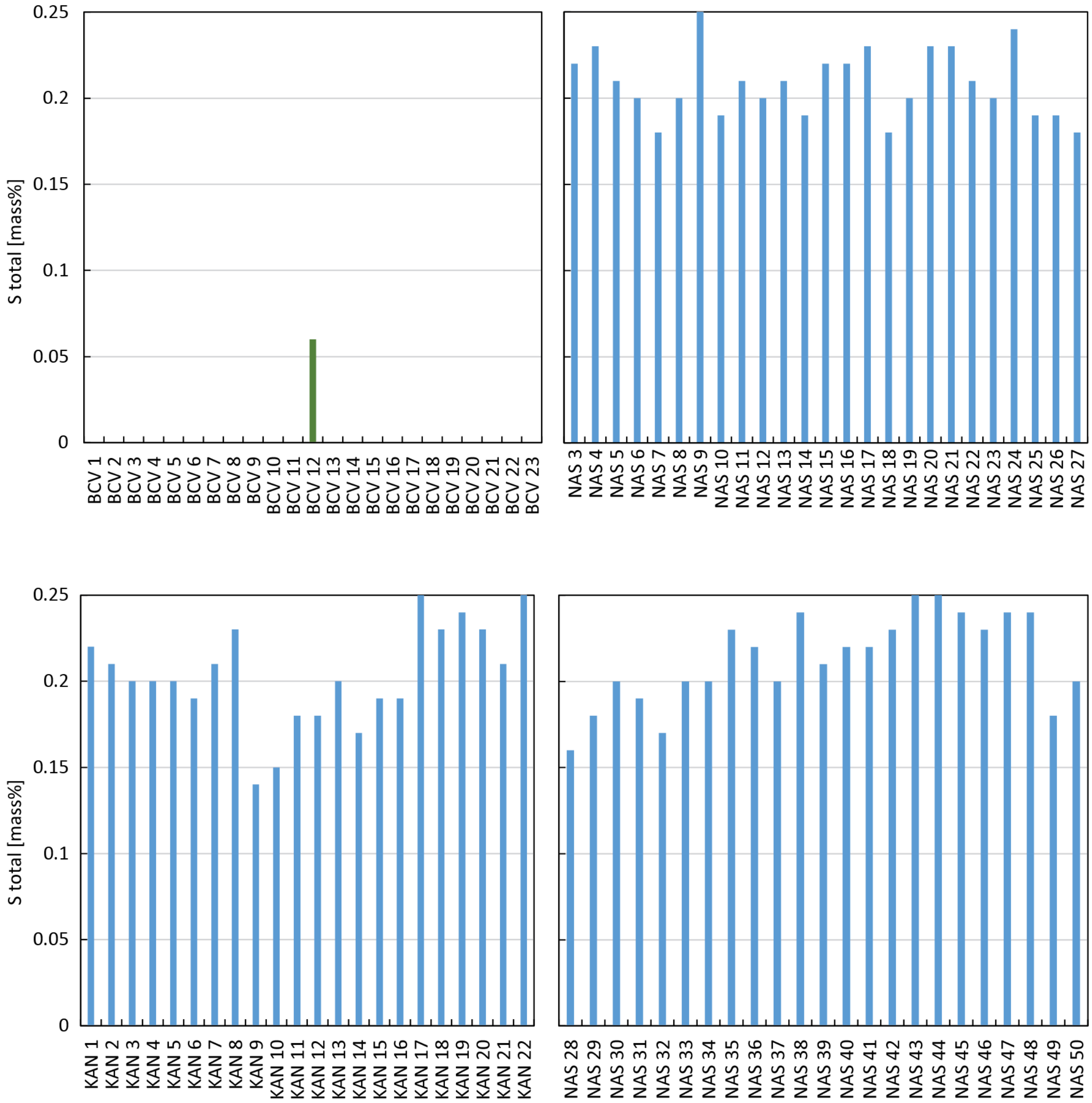

Fig. 6-5: S contents of all GBM samples

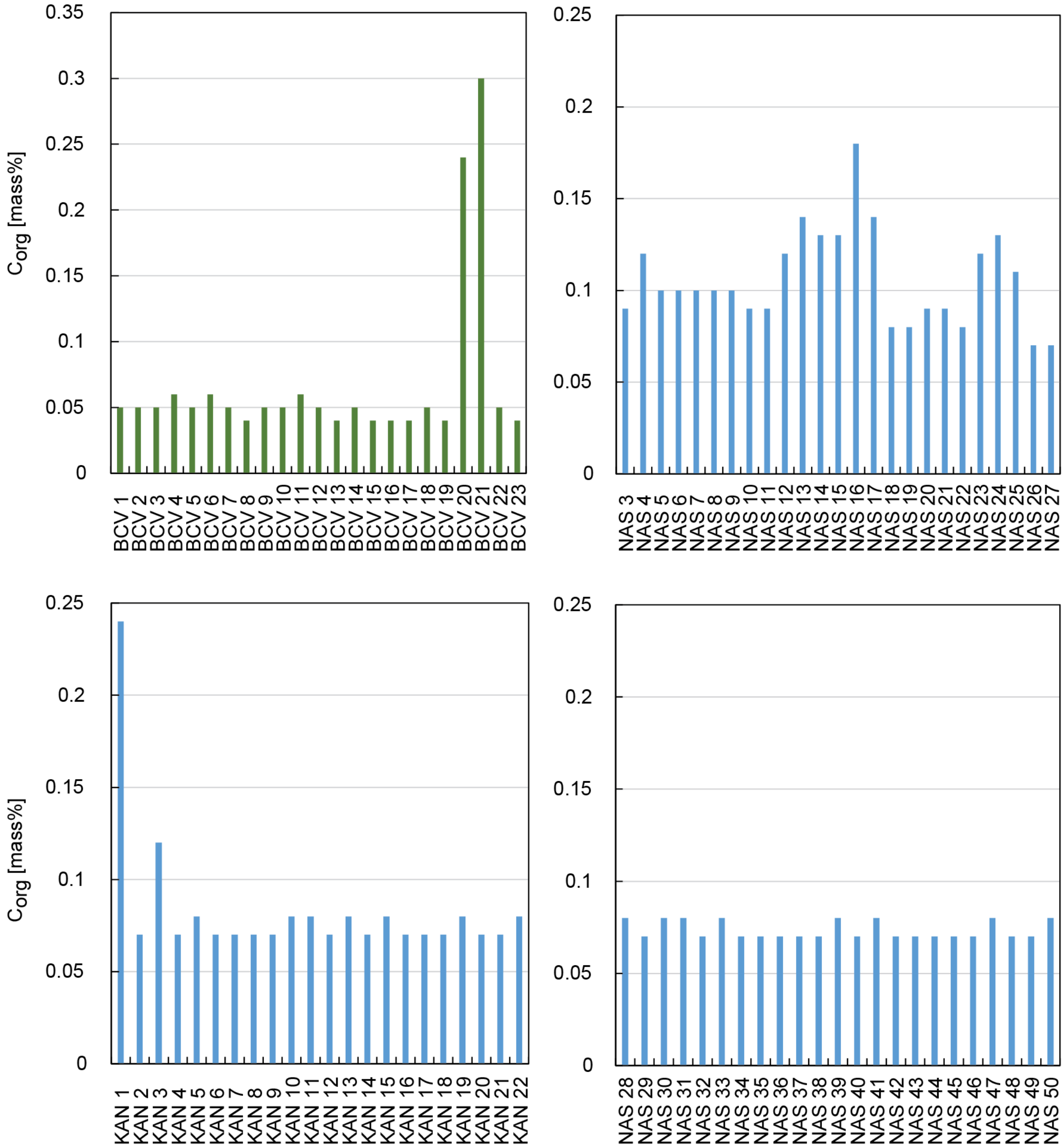

Fig. 6-6: Organic C contents of all GBM samples

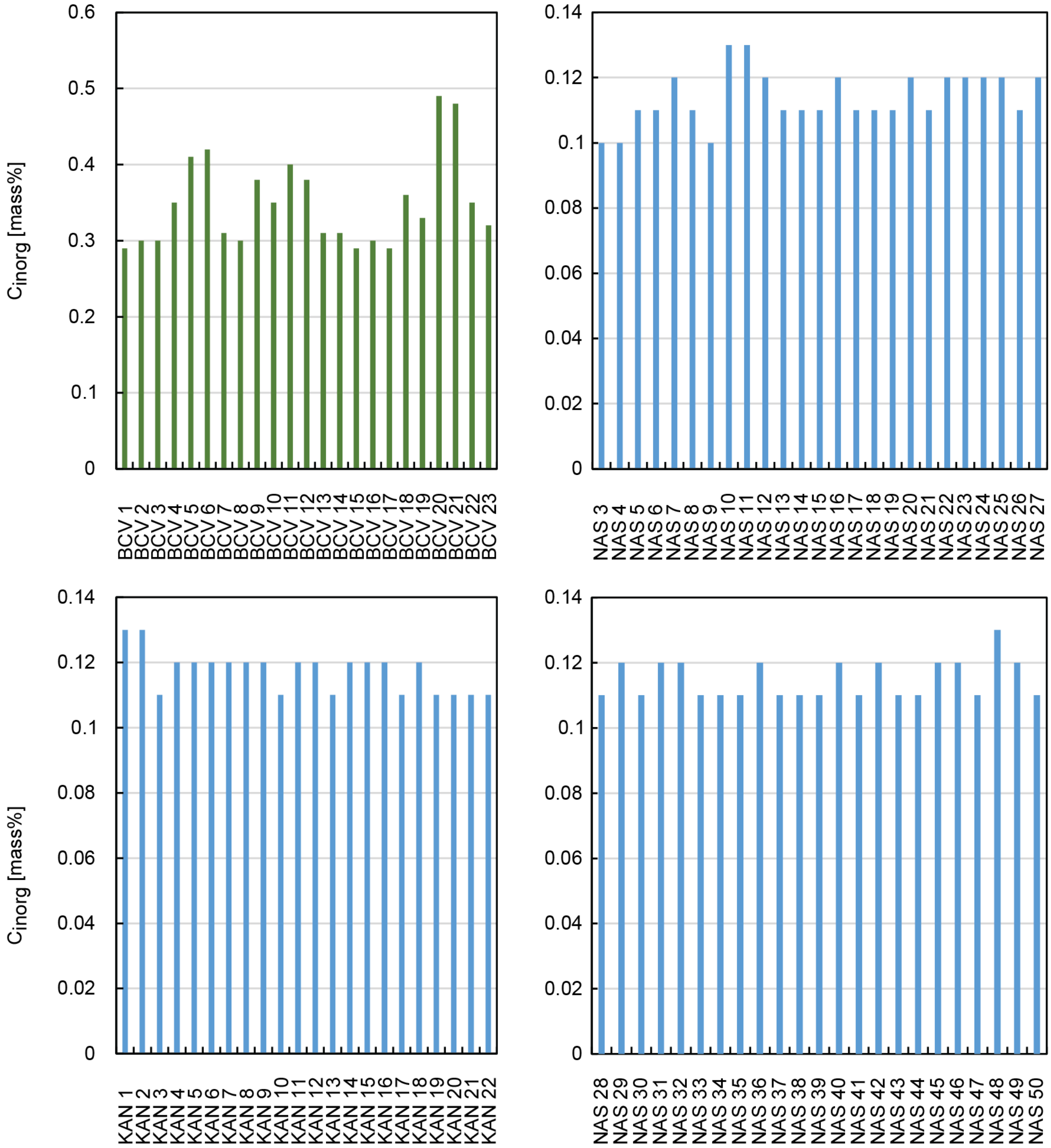

Fig. 6-7: Inorganic C contents of all GBM samples

Note differences in scales between BCV and National® samples

Note that inorganic C was calculated as the difference of total C minus organic C after removal of carbonate minerals by hot HCl solution.

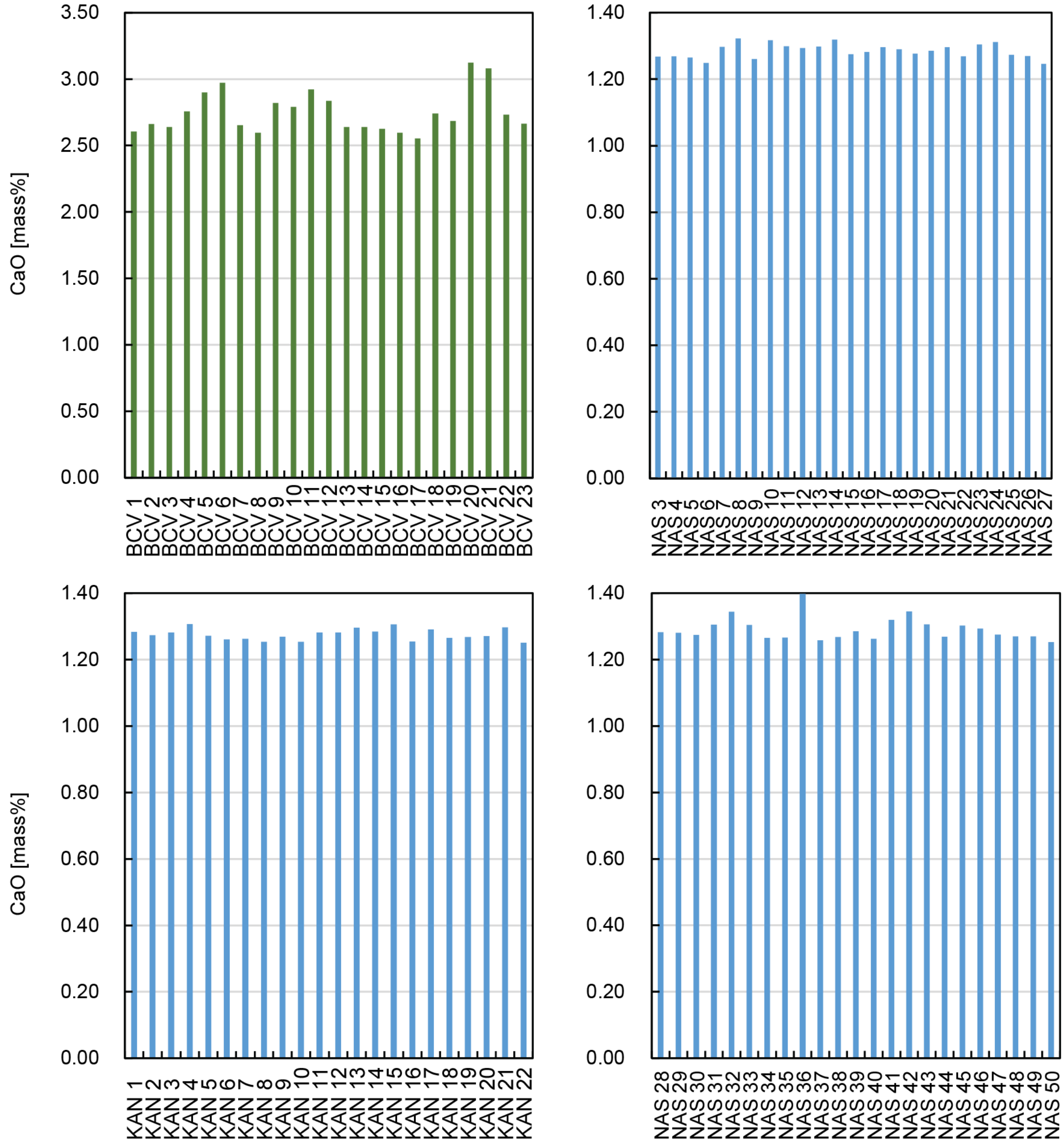

Fig. 6-8: CaO contents of all GBM samples

Note differences in scales between BCV and National® samples

The scatter which can be observed in the different diagrams of course depends on the absolute values. The samples with higher TiO_2 contents (BCV1 – BCV23) also apparently show less scatter compared to samples with lower absolute values in TiO_2. This might result from their lower TiO_2 contents.

As expected, the standard deviation of the samples with higher contents is larger (Tab. 6-1). No significant deviations within a given bentonite material (National® or BCV) were found for TiO_2, Fe_2O_3, and S (determined by LECO analysis; Fig. 6-3, Fig. 6-4, and Fig. 6-5). The National® samples show some scatter of S values which may result from small differences in contents of gypsum and pyrite. For CaO and C-organic values, outliers were identified (Fig. 6-6 and Fig. 6-8).

The TiO_2 contents, for example, show larger visible scatter compared to Fe_2O_3.

Samples BCV 20 and BCV 21 contain more CaO (3.1 mass% compared to about 2.7 mass% for the others), much more organic C (0.25 – 0.3 mass% compared to 0.05 mass% of the others), and more inorganic C (0.49 mass% compared to 0.35 mass% for the others). These differences may indicate a heterogeneity of the material (as delivered) or point to some contamination before sampling, or have another cause. The deviation has to be checked carefully using further mineralogical analysis. Also, sample KAN1 contains much more organic C compared with the others (0.24 mass% compared to < 0.1 mass% for the others). The organic C contents of samples NAS 3 to NAS 27 were also slightly larger compared to the others (about 0.1 mass% compared to 0.07 mass%). This difference, however, is close to the detection limit of the LECO analysis (about 0.02 mass%). A slightly higher CaO value of sample NAS36 was found (1.4 mass% compared to 1.3 mass% for the others) but this difference lies within the accuracy of the method (about 0.1 mass%). K_2O concentrations are on average 0.8 mass % in BCV GBM samples, and slightly less concentrated with on average 0.7 mass % in National Standard® GBM samples. Low concentrations of Na_2O, MnO, and P_2O_5 are present in all GBM samples, and differences in these oxides are low as well.

Tab. 6-1: Average compositions of GBM samples based on XRF and LECO data

	C_{total}	C_{org}	S_{total}	SiO_2	TiO_2	Al_2O_3	Fe_2O_3	MnO	MgO	CaO	Na_2O	K_2O	P_2O_5
Mass	%	%	%	%	%	%	%	%	%	%	%	%	%
BCV 1 - 23	0.42	0.07	< 0.1	56.4	3.3	17.1	15.8	0.2	3.2	2.7	0.1	0.8	0.4
St. Dev.	0.11	0.06		0.19	0.04	0.19	0.24	0.01	0.03	0.15	0.05	0.06	0.01
NAS 3-27	0.22	0.11	0.21	68.8	0.2	19.9	4.2	0.0	1.8	1.3	2.8	0.7	0.0
St. Dev.	0.03	0.03	0.02	0.57	0.01	0.34	0.11	0.00	0.02	0.02	0.06	0.01	0.00
NAS 28-50	0.19	0.07	0.21	67.7	0.2	20.6	4.4	0.0	1.8	1.3	2.9	0.7	0.1
St. Dev.	0.01	0.00	0.03	0.46	0.01	0.27	0.09	0.00	0.02	0.03	0.04	0.02	0.00
KAN 1-22	0.20	0.08	0.20	68.3	0.2	20.2	4.3	0.0	1.8	1.3	2.9	0.7	0.1
St. Dev.	0.04	0.04	0.03	0.34	0.01	0.21	0.07	0.00	0.02	0.02	0.03	0.01	0.00
NAS Avg.	0.20	0.09	0.21	68.3	0.2	20.2	4.3	0.0	1.8	1.3	2.9	0.7	0.1

6.3 Block samples

The main composition of major oxides in the block samples was compared with the average values of the GBM samples ("REF" in Fig. 6-9).

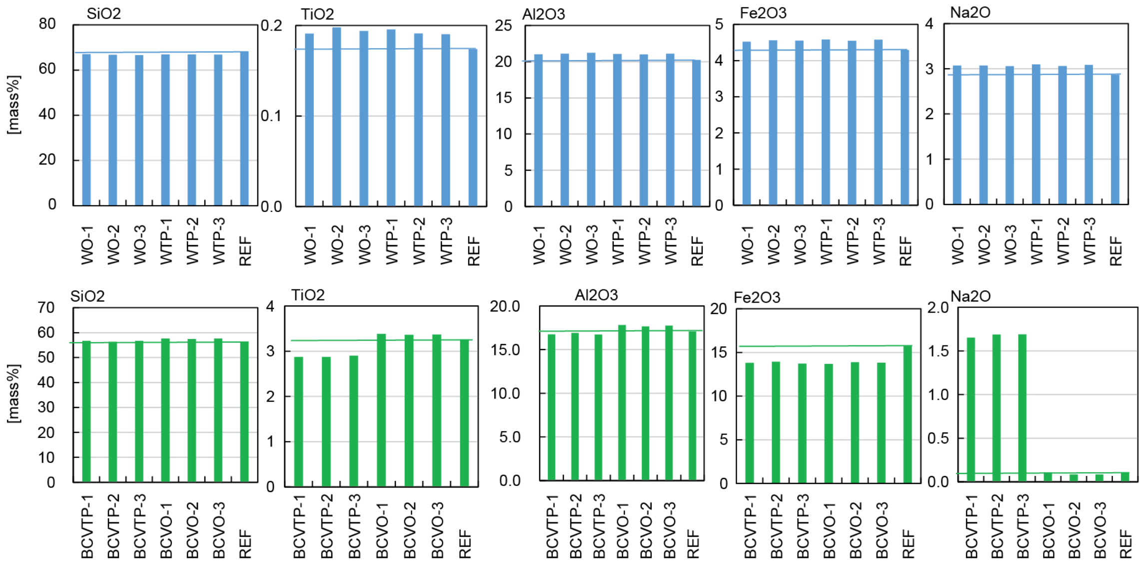

Fig. 6-9: Comparison of the chemical composition of the 12 block samples

WO = National® ordinary block, WTP = National® top block, BCVO = BCV ordinary block, BCVTP = BCV top block.

The National® ordinary block samples and top block samples showed a slightly different composition pointing to the fact that a different material charge was used to produce the blocks. The comparison of all elements and major oxides, however, shows that the differences are comparatively small (Tab. 6-2). The block samples contain a little less SiO_2 (quartz, cristobalite) but about 1 mass% more Al_2O_3 than the GBM, which points to a larger clay and feldspar content. Overall, both materials (GBM and blocks) are homogenous and no differences between the ordinary and top blocks could be found.

All BCV bentonite blocks showed a slightly lower Fe_2O_3 content than that used for BCV GBM, which indicates that the blocks were likely produced using different charges. Larger differences were observed between the top block samples and the ordinary block samples from BCV. Although not identical, the ordinary blocks were still similar to the BCV GBM samples. The top blocks, however, differed significantly. The differences between the ordinary and the top blocks are summarised in Fig. 6-10.

Tab. 6-2: Comparison of the average values of chemical analyses of the National® GBM samples (upper row) with the average values of the National® block samples

	C_{total}	C_{org}	S_{total}	SiO_2	TiO_2	Al_2O_3	Fe_2O_3	MnO	MgO	CaO	Na_2O	K_2O	P_2O_5
Mass	%	%	%	%	%	%	%	%	%	%	%	%	%
NAS GBM avg. (n=70)	0.2	0.1	0.2	68.3	0.2	20.2	4.3	0.0	1.8	1.3	2.9	0.7	0.1
St. Dev.	0.02	0.02	0.02	0.46	0.01	0.27	0.09	0.00	0.02	0.02	0.05	0.01	0.00
NAS blocks (n=6)	0.2	0.1	0.2	66.9	0.2	21.1	4.6	0.0	1.8	1.3	3.1	0.7	0.1

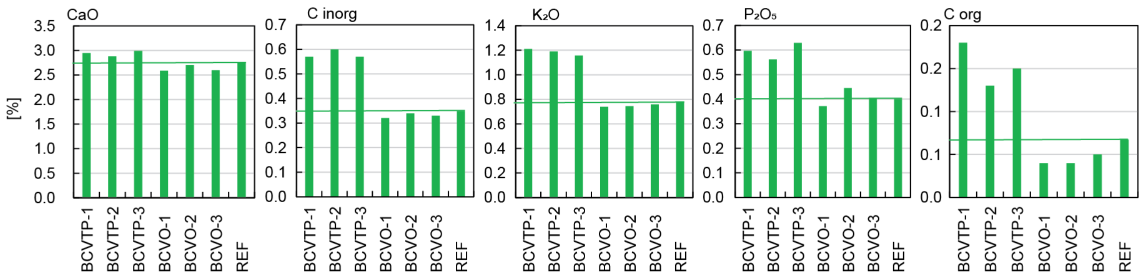

Fig. 6-10: Differences between BCV top and ordinary blocks

The BCV top blocks showed higher inorganic carbon values than the ordinary blocks and the GBM samples but only slightly more CaO, which is interesting because, normally, both parameters are related to the Ca-carbonate content. At the same time, higher K_2O, P_2O_5, and C_{org} values were found in the top blocks compared to the ordinary blocks and bag samples. All values are compared in Tab. 6-3.

Tab. 6-3: Comparison of the chemical composition of all (n=23) BCV GBM samples (BCV, upper row) with top and ordinary blocks

The block values represent the average of three measurements each (n=3)

	C_{total}	C_{org}	S_{total}	SiO_2	TiO_2	Al_2O_3	Fe_2O_3	MnO	MgO	CaO	Na_2O	K_2O	P_2O_5
Mass	%	%	%	%	%	%	%	%	%	%	%	%	%
BCV GBM	0.4	0.1	< 0.1	56.4	3.3	17.1	15.8	0.2	3.2	2.7	0.1	0.8	0.4
St. Dev.	0.11	0.06		0.19	0.04	0.19	0.24	0.01	0.03	0.15	0.05	0.06	0.01
BCV top	0.7	0.2	< 0.1	56.6	2.9	16.8	13.8	0.2	3.2	2.9	1.7	1.2	0.6
BCV ordinary	0.4	0.0	< 0.1	57.6	3.4	17.8	13.8	0.2	3.3	2.6	0.1	0.7	0.4

The differences in chemical composition between the BCV top and ordinary blocks are relevant since both materials are directly in contact to each other and the differences cause chemical gradients which can be investigated further, especially after dismantling.

7 Lessons learned and conclusions

The bentonite components used within the HotBENT benefitted in particular from the experience gained during the FE experiment (Müller et al. 2017 and Garitte et al. 2015).

The following sections highlight specific lessons learned during implementation.

7.1 Blocks

The mineralogy of the bentonite raw material strongly influences the manufacturing of bentonite blocks. During HotBENT, it was observed that the Na-dominated National® 1802 has a different behaviour during compaction than the Ca-Mg-bentonite BCV. Furthermore, the water content of the raw material affects the obtained properties of the final blocks.

The loading tests at GTS showed that the bentonite blocks were stable at the expected conditions relevant for the construction of HotBENT.

The construction of the bentonite block pedestals could be completed as planned without any major complications, highlighting the usefulness of strict geometrical requirements for the blocks.

7.2 GBM

During the manufacturing of the GBM, it was observed that the water content in the raw material strongly affects the water content of the final GBM mixture. This is due to the final GBM consisting of ¼ raw material, but also due to the decrease in the dry density of the compacted pellets along with an increase in water content in the raw material.

The following lessons are drawn from the HotBENT backfilling:

(i) A trend towards decreased backfilling densities was observed over the period of the HotBENT project. This could be related to the wear of the augers.

(ii) The backfilling behaviour of the National® WP1000 and the BCV GBM were different with the BCV GBM characterised by a stronger stickiness. The slightly higher water content of the BCV GBM could be one reason, but similar difficulties regarding the stickiness of the BCV were observed during the manufacturing of the blocks, where similar water content between the National® and BCV materials was used.

(iii) The density calculations rely on the accuracy of the volume estimates and the backfilled mass estimate. Special attention should be paid to the accuracy of those two parameters. Furthermore, the density calculations assume a homogeneous distribution of the GBM. However, observations during the backfilling process highlight the observation reported by the FE experiment (Nagra 2019) that the GBM density behind the augers is highest and that it decreases with an increase in the distance from the augers.

7.3 Summary of baseline characterisation

The report provides reference data and a statistical assessment of the chemical composition of the Wyoming (National Standard®) and BCV bentonites. The Wyoming bentonite samples were quite similar. Obviously, a slightly different material was used for production of the blocks compared to the GBM, but the ordinary and top block materials were similar. In contrast, rather different materials were used for the production of BCV top and ordinary blocks. This finding is of particular interest because both materials are in close contact with each other. The interface of BCV top and ordinary blocks is, therefore, an interesting location for sampling after dismantling of Sector 2.

7.4 Conclusions

All bentonite components (blocks and GBM) used within HotBENT were produced in compliance with the requirements for the National® components.

The production of the blocks was hampered by the differences in the behaviour of the BCV ordinary blocks during production compared to the pre-tests, but all blocks were delivered on time. The production of the GBM and the transport of nearly 200 tonnes of GBM to the GTS were carried out successfully.

The backfilling process and especially the manoeuvring of heavy equipment in confined space could be managed without severe injuries. Ventilation during backfilling was strong enough to provide safe working conditions and to protect the data acquisition systems from bentonite dust.

A summary on the emplaced materials and the achieved dry density for each bentonite block pedestal, but more importantly the dry density overall (including bentonite block pedestal and GBM), is given in Tab. 7-1.

The dry density values can be converted into the effective montmorillonite density using the montmorillonite content described in Section 2.3. This results in an effective montmorillonite density of 1.17 g/cm^3 for Sector 1, 1.15 g/cm^3 for Heater Module 3 and 1.21 g/cm^3 for Heater Module 4.

Tab. 7-1: Summary of bentonite components in HotBENT

		Bentonite		
		Volume	**Dry mass**	**Dry density**
		[L]	[kg]	[g/cm^3]
Heater 1	GBM	11,370	16,846	1.48
	Pedestal	826	1,437	1.74
	Total	12,196	18,282	1.50
Heater 2	GBM	8,070	11,414	1.41
	Pedestal	826	1,445	1.75
	Total	8,896	12,859	1.45
Sector 1	GBM	40,970	58,177	1.42
	Pedestal	1,651	2,881	1.75
	Total	42,621	61,058	1.43
Heater 3	GBM	22,990	32,454	1.41
	Pedestal	826	1,445	1.75
	Total	23,816	33,898	1.42
Sector 2 Wyo	GBM	28,800	40,106	1.39
	Pedestal	826	1,445	1.75
	Total	29,626	41,551	1.40
Heater 4	GBM	17,720	23,637	1.33
	Pedestal	826	1,379	1.67
	Total	18,546	25,016	1.35
Sector 2 BCV	GBM	29,360	40,547	1.38
	Pedestal	826	1,379	1.67
	Total	30,186	41,925	1.39
Sector 2 total	GBM	58,160	80,653	1.39
	Pedestal	1,651	2,824	1.71
	Total	59,811	83,476	1.40
HotBENT total	GBM	99,130	138,829	1.40
	Pedestal	3,302	5,705	1.73
	Total	102,432	144,534	1.41

8 References

Åkesson, M. (2012). Temperature buffer test - Final report. SKB Technical Report TR-12-04.

Dixon D.A., Chandler N.A., & Baumgartner P. (2002). The influence of groundwater salinity and influences on the performance of potential backfill materials. Session IV, paper 9.- Proceedings of the 6th International Workshop on Design and Construction of Final Repositories, Backfilling in Radioactive Waste Disposal, Brussels, Belgium, 11–13 March 2002. ONDRAF/NIRAS, Brussels, Belgium. Transactions, 2002, Bd. 58

ENRESA (2000). Full-scale engineered barriers experiment for a deep geological repository in crystalline host rock, FEBEX Project, European Commission: 403.

Finsterle S., Kober F., & Vomvoris S. (2020). HotBENT - Modelling of Enhanced Pressuration Options. Nagra Arbeitsbericht. NAB 20-020.

Finsterle S., Kober F., & Vomvoris S. (2019). HotBENT: Detailled Design Phase: Additional Study of TH Phenomenological Aspects. Nagra Arbeitsbericht. NAB 19-022.

Fuller, W.B., & Thompson, S.E. (1907). The laws of proportioning concrete. ASCE J. Transport., Vol. 59, pp. 67-143.

García-Siñeriz J.L., & Tuñón S. (2020). HotBent - Experiment plan. Nagra Arbeitsbericht. NAB 19-043.

Garitte, B., Weber, H. P., & Müller, H. R. (2015). Requirements, manufacturing and QC of the buffer components. Nagra Working Report, NAB 15–24, Nagra, Wettingen, Switzerland and EU Project LUCOEX, Deliverable D2.3. www.lucoex.eu.

Gaus, I., Garitte, B., Senger, R., Gens, A., Vasconcelos, R., Garcia-Sineriz, J-L., Trick, T., Wieczorek, K., Czaikowski, O., Schuster, K., Mayor, J. C., Velasco, M., Kuhlmann, U. & Villar M.V. (2014): The HE-E Experiment: Lay-out, interpretation and THM modelling. Nagra Arbeitsbericht NAB 14-53. PEBS deliverable D2.2-11 and D3.2-2.

Grim, R.E. & Güven, N. (1978). Bentonites, Geology, Mineralogy, Properties and Uses, Development in Sedimentology. Vol. 24, Elsevier, Amsterdam.

Hausmannová, L., Hanusová, I., and Dohnálková, M. (2018). Summary of the research of czech bentonties for use in the deep geological repository – up to 2018. SÚRAO Technical report 309/2018/ENG

Hoffmann, C., Alonso, E.E. & Romero, E. (2007). Hydro-mechanical behaviour of bentonite pellet mixtures. Physics and Chemistry of the Earth 32, 832-849.

IAEA (2003). Scientific and Technical Basis for the Geological Disposal of Radioactive Wastes, Technical Reports Series No. 413, IAEA, Vienna

Jenni, A., & Köhler, S. (2015). WP 2 – Full-Scale emplacement (FE) experiment – Report on the construction, testing and commissioning of the emplacement equipment. Lucoex report D2:D04

Kaufhold, S., Dohrmann, R., & Klinkenberg, M. (2010). Water-Uptake Capacity of Bentonites. Clays Clay Miner. 58, 37–43.

Kiviranta, L., & Kumpulainen, S. (2011). Quality Control and Characterization of Bentonite Materials.

Kober, F., Vomvoris, S., & Finsterle, S. (2018). HotBENT: Preliminary Design Study - Overview of Results. Nagra Arbeitsbericht. NAB 17-029.

Kober F., García-Siñeriz J.L., Villar M.V., Lanyon G.W., Cloet V., Mäder U., Wersin P., Leupin O. X., Sellin P., Gens A., & Schneeberger R. (2021). FEBEX-DP Synthesis Summary of the Full-Scale Engineered Barriers Experiment – Dismantling Project. Nagra Technischer Bericht. NTB 17-01.

Kober, F., Schneeberger, R., & Manukyan, E., (in prep.). HotBENT instrumentation: As built report. Nagra Arbeitsbericht NAB 22-008.

Lanyon B., Schneeberger R., & Kober F. (2020). HotBENT Geosphere Characterisation and Instrumentation Plan. Nagra Arbeitsbericht. NAB 20-019.

Leupin O. X. (ed.), Birgersson M., Karnland O., Korkeakoski P., Sellin P., Mäder U., & Wersin P. (2014). Montmorillonite sTability under near-field conditions. Nagra Technischer Bericht. NTB 14-12.

Müller, H.R., Garitte, B., Vogt, T., Köhler, S., Sakaki, T., Weber, H., & Cloet, V. (2017). Implementation of the full-scale emplacement (FE) experiment at the Mont Terri rock laboratory. Swiss Journal of Geosciences, 110(1), 287-306.

Nagra (2019). Implementation of the Full-scale emplacement Experiment at Mont Terri: Design, Construction and Preliminary Results. Nagra Technischer Bericht. NTB 15-02.

NEA (1995). The Environmental and Ethical Basis of the Geological Disposal of Long-Lived Radioactive Waste

Proctor, R. (1933). Fundamental principles of soil compaction. Engineering news-record, 111(13).

Sellin, P., & Leupin, O.X. (2013). The Use of Clay as an Engineered Barrier in Radioactive-Waste Management a Review. Clays Clay Miner. 61, 477–498.

Seiphoori A. (2015). Thermo-hydro-mechanical characterisation and modelling of Wyoming granular bentonite. Nagra Technischer Bericht. NTB 15-05.

Schneeberger R., Kober F., Lanyon G.W., Spillmann T., & Blechschmidt I. (2019). Grimsel Test Site: Revisiting the site-specific geoscientific knowledge. Nagra Technischer Bericht. NTB 19-01.

Schneeberger R., Kober F., Dorrer R., Treuthardt M., Baer T., & Dorrer A.-S. (2021). HotBENT Gallery and site preparation report. Nagra Arbeitsbericht. NAB 20-018.

Schneeberger R., & Rouspoulou V. (2021). HotBENT: Geological characterisation of the enhanced geosphere pressurization boreholes. Nagra Arbeitsbericht. NAB 21-028.

Schneeberger, R., & Kober, F. (2022). HotBENT: Cementitious materials requirements and as-built characteristics. Nagra Arbeitsbericht NAB 22-006.

Svemar, C., Johannesson, L.-E., Grahm, P., Svensson, D., Kristensson, O., Lönnqvist, M., & Nilsson, U. (2016). Prototype Repository: Opening and Retrieval of Outer Section of Prototype Respository at Äspö Hard Rock Laboratory: Summary Report. TR-13-22, Svensk Kärnbränslehantering AB, 2016.

Wersin, P., Johnson, L.H., & McKinley, I.G. (2007). Performance of the bentonite barrier beyond 100ºC: A critical review. Physics and Chemistry of the Earth 32, 780-788.